HDL-CR-81-216-1
February 1981

Development of a Fluidic, Hydraulic Servovalve

Prepared by
D. N. Wormley, D. Lee, and K-M. Lee
Massachusetts Institute of Technology
Ambridge, MA 02139

Under contract
DAAG-39-77-C-0216

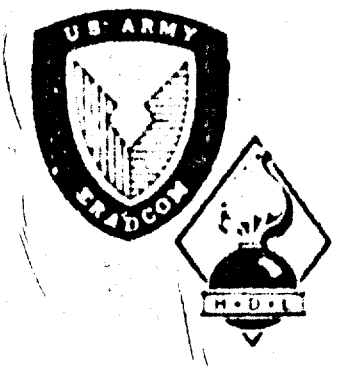

U.S. Army Electronics Research
and Development Command
Harry Diamond Laboratories
Adelphi, MD 20783

The findings in this report are not to be construed as an official Department of the Army position unless so designated by other authorized documents.

Citation of manufacturers' or trade names does not constitute an official indorsement or approval of the use thereof.

Destroy this report when it is no longer needed. Do not return it to the originator.

UNCLASSIFIED

SECURITY CLASSIFICATION OF THIS PAGE (When Data Entered)

(18) HDL, HDL

(19) REPORT DOCUMENTATION PAGE

READ INSTRUCTIONS BEFORE COMPLETING FORM

1. REPORT NUMBER: HDL-CR-81-216-1, 80-1	2. GOVT ACCESSION NO.: AD-A100883
3. RECIPIENT'S CATALOG NUMBER: rept.	
4. TITLE (and Subtitle): (6) DEVELOPMENT OF A FLUIDIC, HYDRAU... SERVOVALVE.	5. TYPE OF REPORT & PERIOD COVERED: FINAL, 1977 — 1980
	6. PERFORMING ORG. REPORT NUMBER: ...-Co-1
7. AUTHOR(s): (10) D. N. Wormley, D. Lee, K-M. Lee (15)	CONTRACT OR GRANT NUMBER(s): AG+39-77-C-0216
9. PERFORMING ORGANIZATION NAME AND ADDRESS: Massachusetts Institute of Technology, Cambridge, MA 02139	10. PROGRAM ELEMENT, PROJECT, TASK AREA & WORK UNIT NUMBERS: Prog. Ele.: 6.11.02.A
11. CONTROLLING OFFICE NAME AND ADDRESS: U.S. Army Harry Diamond Laboratories, 2800 Power Mill Road, Adelphi, MD 20783 (11)	12. REPORT DATE: FEB[illegible]981
	13. NUMBER OF PAGES: 56
14. MONITORING AGENCY NAME & ADDRESS (if different from Controlling Office): (12) 58	15. SECURITY CLASS. (of this report): UNCLASSIFIED
	15a. DECLASSIFICATION/DOWNGRADING SCHEDULE

16. DISTRIBUTION STATEMENT (of this Report)

Approved for public release; distribution unlimited.

17. DISTRIBUTION STATEMENT (of the abstract entered in Block 20, if different from Report)

18. SUPPLEMENTARY NOTES (16)

HDL Project: A41134
DRCMS Code: 611102.H.440011
DA Project: 1L161102AH44

19. KEY WORDS (Continue on reverse side if necessary and identify by block number)

Servovalve
Laminar Proportional Amplifier
Fluidic Gain Block

20. ABSTRACT (Continue on reverse side if necessary and identify by block number)

This study focuses upon the analysis, design and experimental evaluation of a hydraulic servovalve constructed from laminar proportional fluid amplifiers and resistance feedback elements. A servovalve has been developed in which the pressure/flow characteristics can be contoured to match a specific application through appropriate design of the proportional amplifiers and selection of the feedback elements.

DD FORM 1 JAN 73 1473 EDITION OF 1 NOV 65 IS OBSOLETE

UNCLASSIFIED 220 600

SECURITY CLASSIFICATION OF THIS PAGE (When Data Entered)

20. Abstract (Cont'd)

A set of design equations have been derived to select the appropriate feedback elements. From the design procedures, two valve configurations have been constructed and tested. Experimental evaluations of the two configurations in terms of static pressure and flow gains and dynamic response have agreed closely with analyses.

CONTENTS

FIGURES

TABLES

1. INTRODUCTION

Hydraulic control systems are widely used in applications where high force levels, fast response and high power to weight ratios are desired. Applications requiring these features include the positioning of aerodynamic control surfaces, precision control of machine tools, marine control equipment and mobile equipment control systems.

The primary power modulation element utilized in high performance hydraulic servosystems are servovalves. These valves are typically constructed as several stages with initial stages consisting of flapper nozzle or jet pipe valves and final stages employing sliding plate or spool valves. A final stage flow control spool valve is illustrated in Figure 1 with the output pressure/flow characteristics typical of a commercial spool valve.[1]

In electrohydraulic servovalves an electrical transducer such as a torque motor or voice coil is coupled with an initial valve stage so that an electrical input can modulate the valve. Valves have been developed also with direct mechanical modulation of the first stage and in the last few years several development efforts have led to valves which accept low level fluidic inputs.[2]

The classes of valves cited above may have many different combinations of input and first stage elements. However in almost all commercial units the final power level modulation stages consist of sliding spool or plate elements. The moving mechanical elements in these valves are associated with a sensitivity to contamination and requirements for tight manufacturing tolerances which result in a significant fraction of valve cost.

The high reliability, insensitivity to extreme environments and low cost associated with no moving part fluidic elements and the potential for weight and size reduction in comparison to conventional valves are attractive features for servovalves. In applications where these attributes are

---

[1] J. F. Blackburn et al., Fluid Power Control, The M.I.T. Press, Cambridge, MA (1960).

[2] R. Deadwyler, Two Stage Servovalve Development Using a First-Stage Fluidic Amplifier, Harry Diamond Laboratories, HDL-TM-80-21 (July 1980).

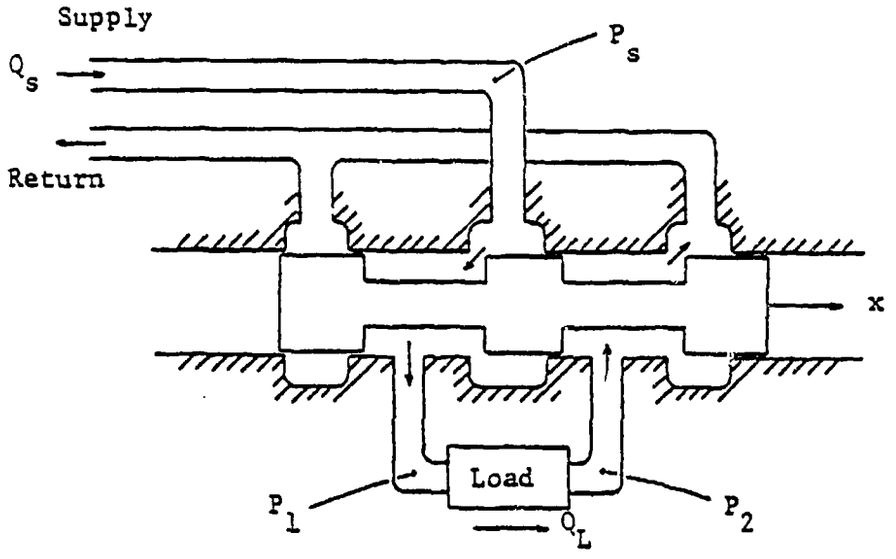

(a) Valve schematic

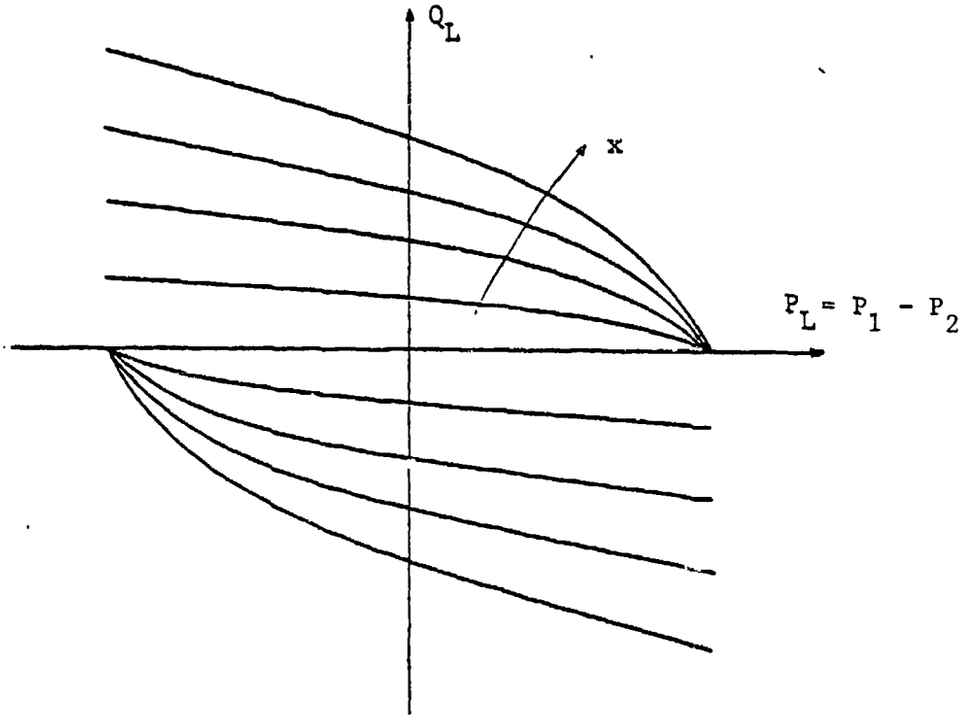

(b) Valve characteristics

Figure 1. Closed center spool valve.

important such as in aircraft, marine and ground vehicle control systems and where the quiescent power drain associated with open-center fluid valves can be accommodated, fluidic servovalves have high potential.

This study focuses upon the conceptualization, analysis, design and experimental evaluation of a hydraulic servovalve constructed from laminar, proportional fluidic elements and resistance feedback elements. The basis for the development is the laminar proportional amplifier[3] (LPA). For the laminar proportional element, the static and dynamic characteristics are well documented, procedures are available to aid in the design of multi-stage amplifier systems[4] and standardized manufacturing techniques have been developed.[5] With the use of LPA elements as a basic building block, a servovalve has been developed in which the pressure/flow characteristics can be contoured to match a specific application through the appropriate design of the proportional amplifiers and selection of the feedback elements. In the development a set of design equations is derived to select the appropriate feedback elements. By the design procedures two valve configurations have been constructed and tested. Experimental evaluations of static pressure and flow gains and dynamic response for the two configurations have agreed closely with the analyses.

2. SERVOVALVE CONFIGURATION DEVELOPMENT

2.1 Laminar Proportional Amplifier Gain Block

The basis for the servovalve development is the laminar proportional fluidic amplifier. Several laminate designs have been developed

---

[3] F. M. Manion and T. M. Drzewiecki, Analytical Design of Laminar Proportional Amplifiers, Proceedings of the HDL Fluidic State-of-the-Art Symposium, Vol. 1, Harry Diamond Laboratories (October 1974).

[4] T. M. Drzewiecki, et al., Computer Aided Design Procedure for Laminar Fluidic Systems, Journal of Dynamic Systems, Measurement and Control, Vol. 97, No. 4 (1975).

[5] L. E. Scheer et al., Manufacturing Techniques for Producing High Quality Fluidic Laminates in Production Quantities, 20th Anniversary of Fluidics Symposium, ASME (November 1980).

including the 3.1.1.8 design shown in Figure 2 which is used in this study. These laminates may be coupled together to form multistage proportional gain blocks.[6] A three stage block has been assembled as described in Section 3. The proportional multistage gain block is represented schematically in Figure 3 with its nondimensional output characteristics illustrated in Figure 4. The output pressure/flow characteristics of the gain block can be represented quite accurately as shown in Figure 4 with the following expression:

$$\frac{Q_L}{Q_{Ls}} = \tanh\left[\frac{P_{cd}}{P_{cds}}\right] - \frac{P_{od}}{P_{ods}} \qquad (1)$$

where

Q_L = output load flow
P_{od} = amplifier output pressure differential
P_{cd} = amplifier input pressure differential
Q_{Ls} = saturation output load flow
P_{ods} = saturation amplifier output pressure differential

and where the saturation control pressure is defined:

$$P_{cds} = \frac{P_{ods}}{K_p} = \frac{Q_{Ls}}{K_q} \qquad (2)$$

with the incremental amplifier static pressure gain (K_p) and flow gain (K_q) defined as

$$K_p = \left.\frac{\partial P_{od}}{\partial P_{cd}}\right|_{Q_L = 0} \qquad (3)$$

$$K_q = \left.\frac{\partial Q_L}{\partial P_{cd}}\right|_{P_{od}=0} \qquad (4)$$

---

[6] D. Lee and D. N. Wormley, Multistage Hydraulic Summing and Signal Processing Amplifiers and Fluidic Input Servovalve Development, Harry Diamond Laboratories, HDL-CR-76-233-1 (1976).

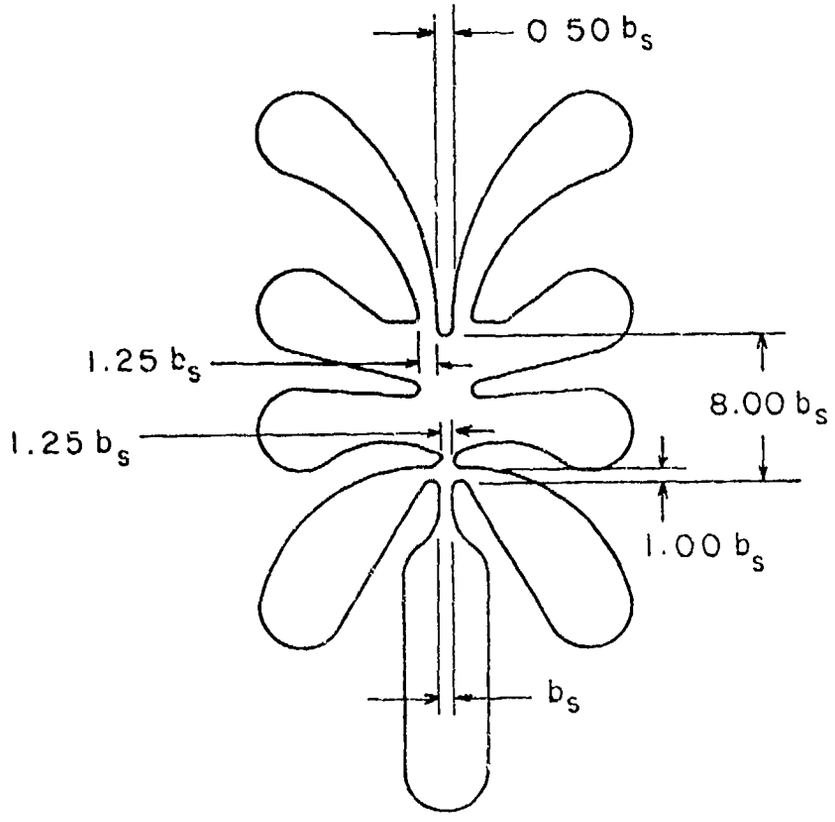

Figure 2. Scaled drawing of HDL 3.1.1.8 laminate.

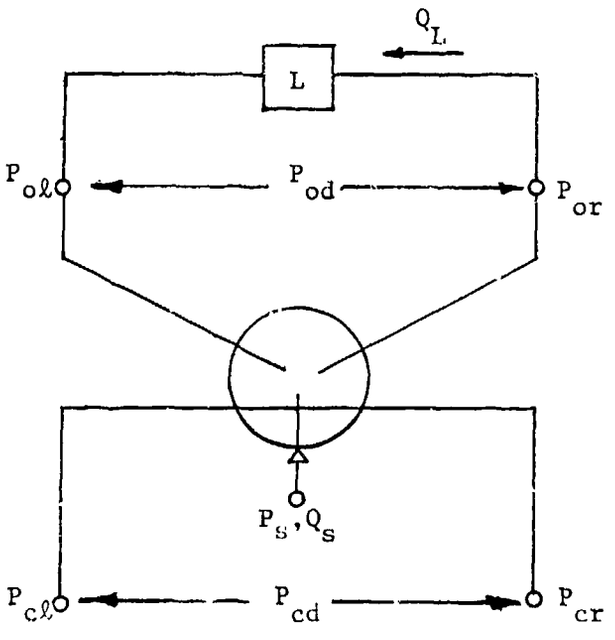

Figure 3. Multistage amplifier configuration.

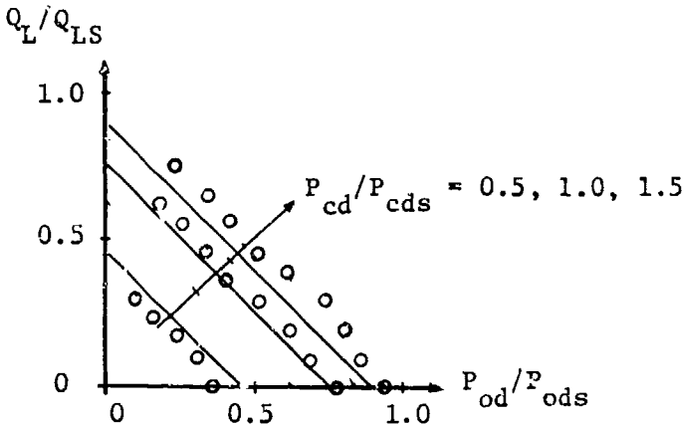

(a) Tanh function approximation of amplifier output characteristics.

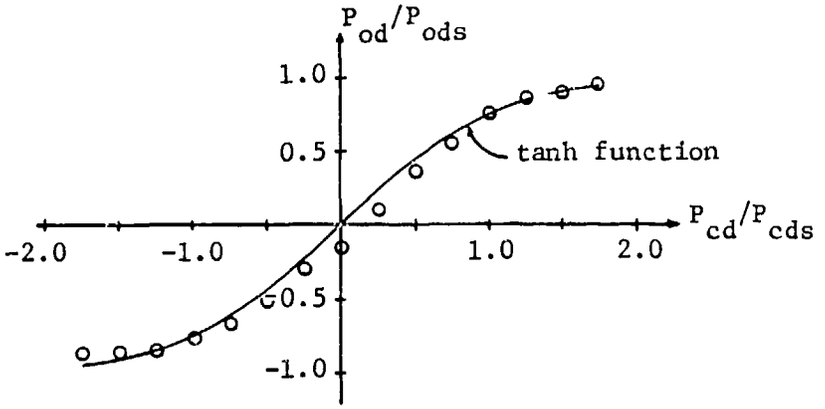

(b) Amplifier pressure gain.

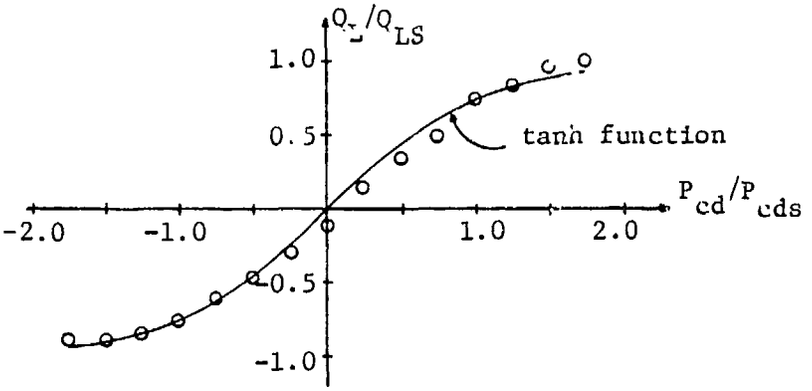

(b) Amplifier flow gain.

Figure 4. Multistage amplifier output characteristics.

and where the incremental quantities K_p and K_q are related by the incremental amplifier flow/pressure characteristic:

$$K_{qp} = \left.\frac{\partial Q_L}{\partial P_{od}}\right|_{P_{cd}=\text{constant}} = \frac{K_q}{K_p} \qquad (5)$$

2.2 Servovalve Configuration

The basic gain block output pressure/flow characteristics described by equation (1), and shown in Figure 4 are relatively linear with respect to the output pressure/flow characteristic for a specified value of input pressure differential. The gain block output characteristics have a high sensitivity of output flow to output pressure. To achieve the typical spool valve flow control characteristics shown in Figure 1, modification of the gain block characteristics is required so that the sensitivity of output flow to output pressure is significantly reduced. The desired modification can be achieved by using feedback principles. The conceptual development of a fluidic servovalve is illustrated in Figure 5 where the influence of positive pressure feedback and negative flow feedback is illustrated.

In Figure 5a, the basic proportional amplifier is augmented with input resistors R_i and pressure feedback resistors R_{fp}. As a differential input signal (P_{id}) is applied to the configuration and pressure develops across the load (P_{od}), this pressure is fed back through R_{fp} to increase the differential pressure (P_{cd}) at the amplifier control ports and increase the load pressure. This positive pressure feedback alters the slope of the output pressure/flow characteristic and modifies the intercept of the characteristics on the output pressure axis as shown in the figure.

In Figure 5b, the proportional amplifier is augmented with a flow sensing resistor R_Q, flow feedback resistors R_{fq} and input resistors R_i. As an input pressure differential (P_{id}) is applied and flow develops

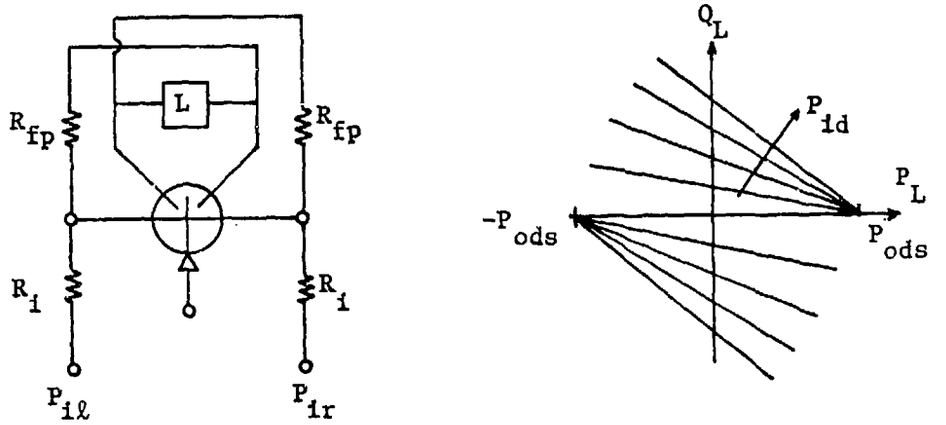

(a) Proportional amplifier with positive pressure feedback

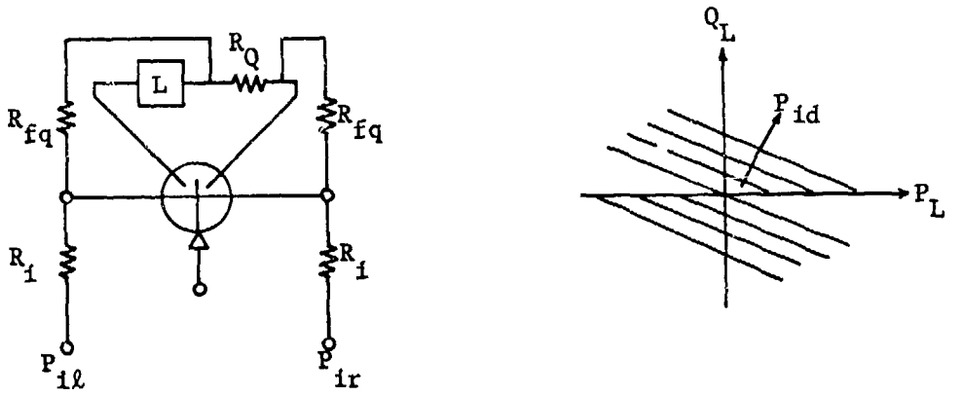

(b) Proportional amplifier with negative flow feedback

P_L = Pressure drop across load

Q_L = Output load flow

$P_{id} = P_{il} - P_{ir}$ = Servovalve input pressure differential

R_{fp} = Pressure feedback resistance

R_{fq} = Flow feedback resistance

R_i = Servovalve input resistance

R_Q = Flow sensing resistor

Figure 5. Fluidic servovalve development.

through the load, a pressure drop occurs across the flow sensing resistor. This pressure drop is fed back through resistors R_{fq} to decrease the pressure differential (P_{cd}) at the amplifier control port and reduce the flow to the load. This negative flow feedback reduces the sensitivity of the output flow to output pressure and generates a flow control type of characteristic. When both pressure and flow feedback features are combined the valve configuration of Figure 6 is obtained. With the appropriate selection of feedback elements the characteristics of flow or pressure control servovalves may be obtained. The basic configuration depicted in Figure 6 is analyzed in the following sections.

2.3 Servovalve Static Characteristics

The static characteristics of the servovalve configuration may be derived by combining the description of the gain block given in equation (1) with the resistance element characteristics using flow and pressure summation circuit analysis laws. In the derivation, it is assumed that feedback and input resistance elements are linear.

By applying flow summation at the right and left amplifier control ports in Figure 6, the following equation may be derived:

$$\frac{P_{i\ell} - P_{ir}}{R_i} + \frac{P_{or} - P_{o\ell}}{R_{fp}} + \frac{P_{o\ell'} - P_{or}}{R_{fq}} = \frac{P_{c\ell} - P_{cr}}{R'} \qquad (6)$$

where each pressure is identified in Figure 6 and where R' is the parallel combination of R_i, R_a, R_{fq} and R_{fp} with

R_i = servovalve input resistance
R_a = amplifier control port input resistance
R_{fq} = flow feedback resistance
R_{fp} = pressure feedback resistance

By noting the relationships

$$P_{id} = P_{i\ell} - P_{ir} \qquad (7)$$

$$P_{o\ell'} - P_{o\ell} = P_L \qquad (8)$$

$$P_{or} - P_{o\ell'} = R_Q Q_L \qquad (9)$$

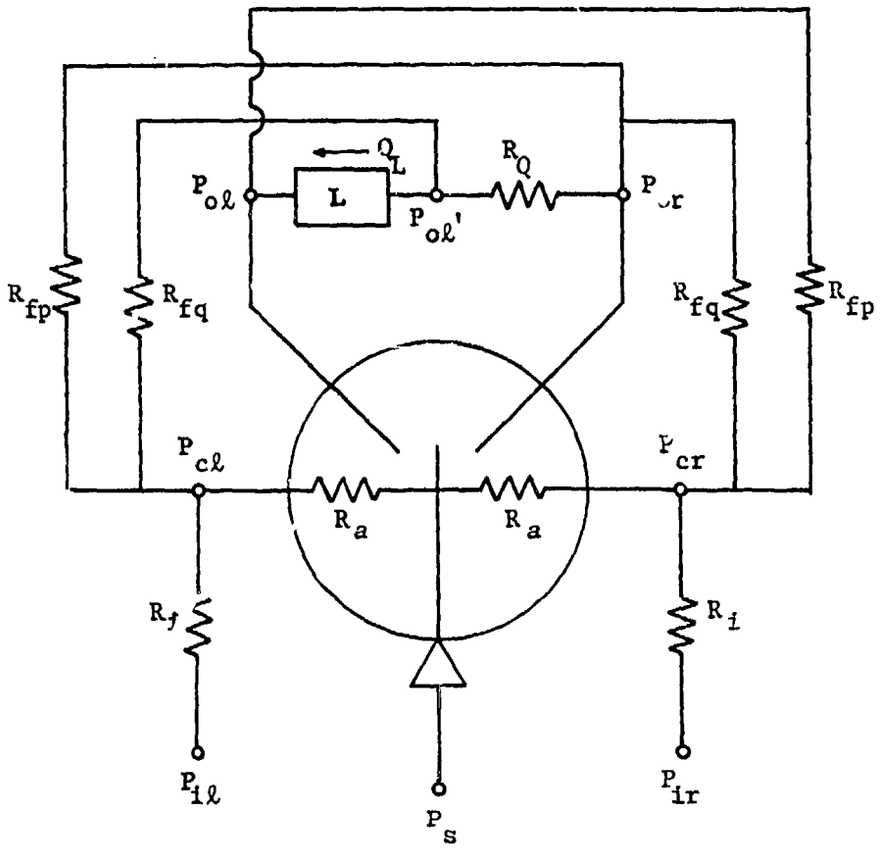

Figure 6. Fluidic servovalve schematic.

where

R_Q = flow sensing resistor

Q_L = output load flow

and defining the maximum output load flow Q_{Lm} and maximum pressure drop P_{Lm} across the load as

$$Q_{Lm} = \frac{K_q}{1 + K_{qp} R_a} P_{cds} \tag{10}$$

$$P_{Lm} = K_p P_{cds} \tag{11}$$

equations (1) and (6) may be combined to yield

$$\bar{Q}_L + \bar{P}_L = \tanh[\alpha \bar{P}_{id} + \beta \bar{Q}_L + \gamma \bar{P}_L] \tag{12}$$

where

$\bar{P}_{id} = P_{id}/P_{idm}$

$\bar{Q}_L = Q_L/Q_{Lm}$

$\bar{P}_L = P_L/P_{Lm}$

with P_{idm} = maximum servovalve input pressure differential

Equation (12) is the general servovalve relationship between the output pressure/flow characteristic and the input control pressure. The nonlinear, nondimensional equation is characterized by three parameters:

$$\alpha = \frac{R'}{R_i} \frac{P_{idm}}{P_{cds}} = \frac{R'}{R_i} \frac{K_q P_{idm}}{(1 + K_{qp} R_Q) Q_{Lm}} \tag{13}$$

$$\beta = \frac{R' K_q R_Q}{1 + K_{qp} R_Q} \left[\frac{1}{R_{fp}} - \frac{1}{R_{fq}}\right] \tag{14}$$

$$\gamma = \frac{K_p R'}{R_{fp}} \tag{15}$$

The coefficient α is related to the input pressure gain while β and γ are related to the flow and pressure feedback coefficients. The variable $\bar{P}_{id}$ varies from 0 to 1 and parametrerizes the $\bar{P}_L/\bar{Q}_L$ output characteristic in terms of nondimensional input pressure.

The valve blocked load pressure is derived from equation (12) by setting $\bar{Q}_L = 0$ and may be written as

$$\frac{1}{2} \ell n\left[\frac{1 + \bar{P}_L}{1 - \bar{P}_L}\right] - \gamma\bar{P}_L = \alpha\bar{P}_{id} \qquad (16)$$

while the valve no load flow may be derived from equation (12) by setting $\bar{P}_L = 0$ to obtain

$$\frac{1}{2} \ell n\left[\frac{1 + \bar{Q}_L}{1 - \bar{Q}_L}\right] - \beta\bar{Q}_L = \alpha\bar{P}_{id} \qquad (17)$$

The blocked load pressure equation (16) and no load flow equation (17) are plotted as a function of input pressure in Figures 7 and 8. The blocked load pressure increases as the input pressure increases and as the parameter γ is increased corresponding to a reduction in the pressure feedback resistor R_{fp}. The no load output flow increases with increasing input pressure and increasing values of β. The value of β may be positive ($R_{fp} < R_{fq}$) or negative ($R_{fq} < R_{fp}$) depending upon the values of the pressure and flow feedback resistors.

Values of positive β increase the flow while values of negative β decrease the flow for a given level of control pressure.

The complete valve characteristics computed from equation (12) are shown in Figure 9 for selected values of α, β and γ. These curves show that small values of α and β generate characteristics that are similar to those of a flow control valve. As α is reduced the flow curves become a more linear function of input pressure. As α is increased the valve characteristics tend to approach those of a pressure control valve. From plots such as those generated from equation (12) a valve may be designed by selecting appropriate values of α, β and γ to have characteristics similar to those of either a conventional pressure or flow

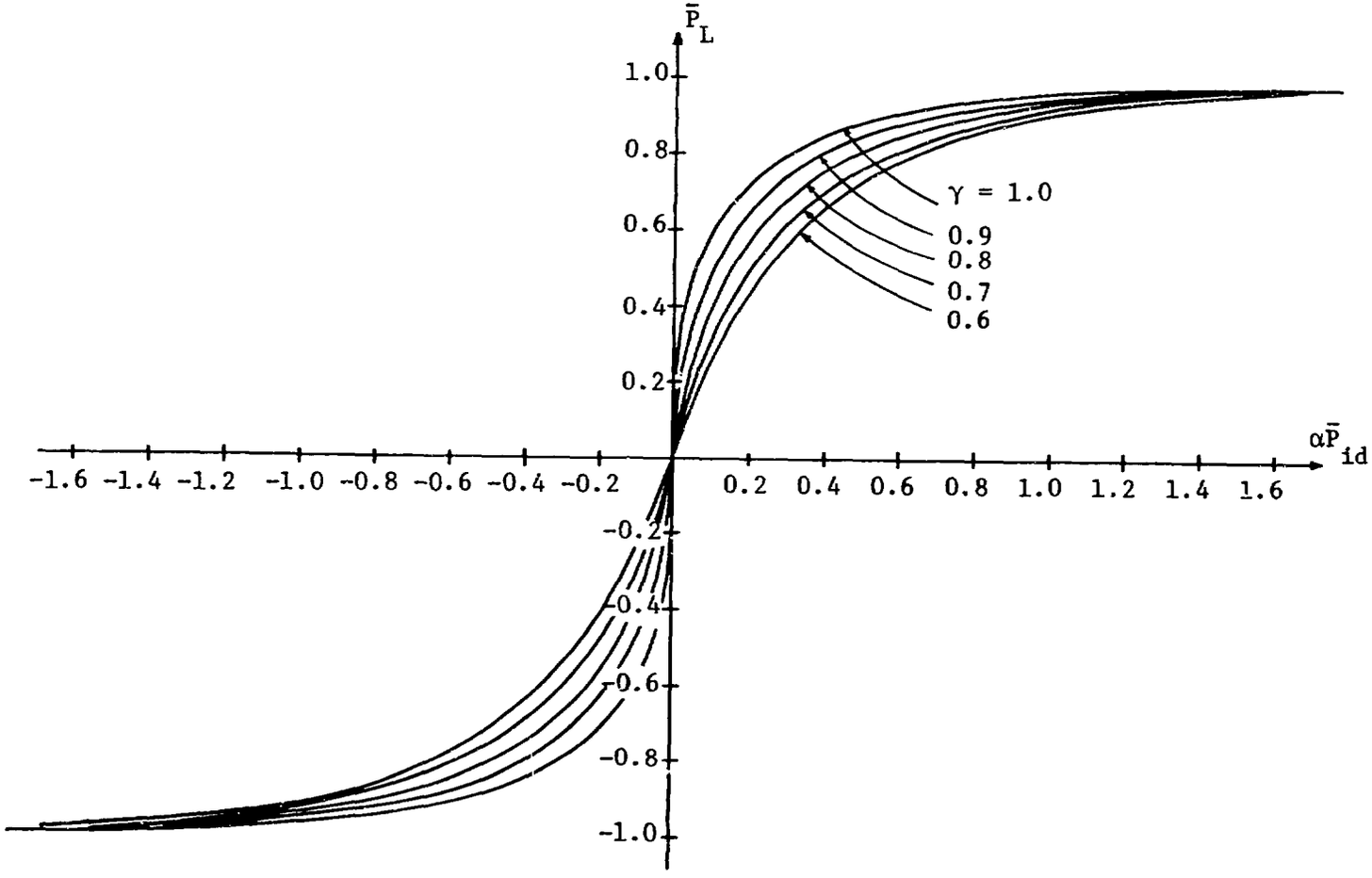

Figure 7. Servovalve blocked load pressure.

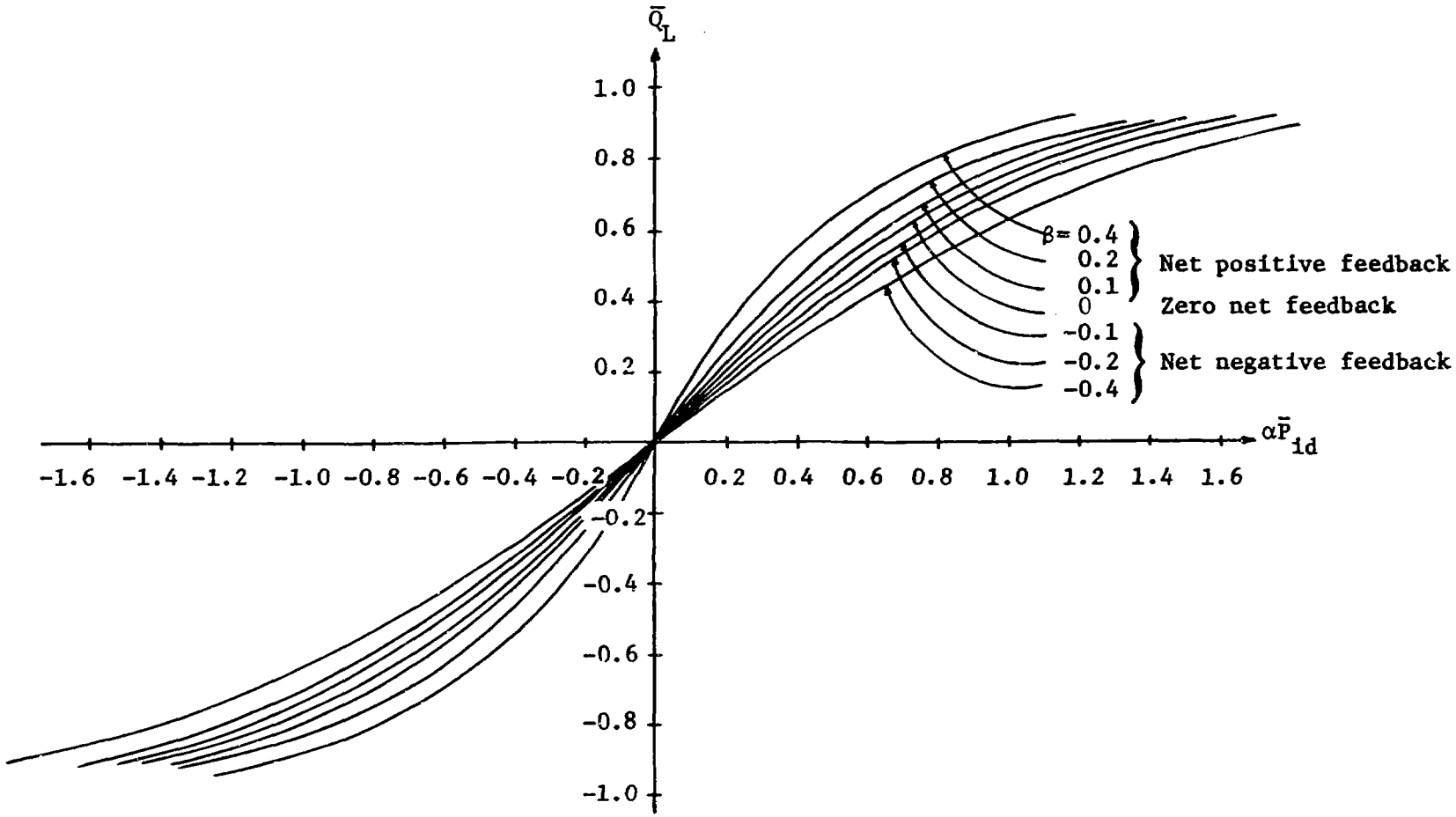

Figure 8. Servovalve no load flow.

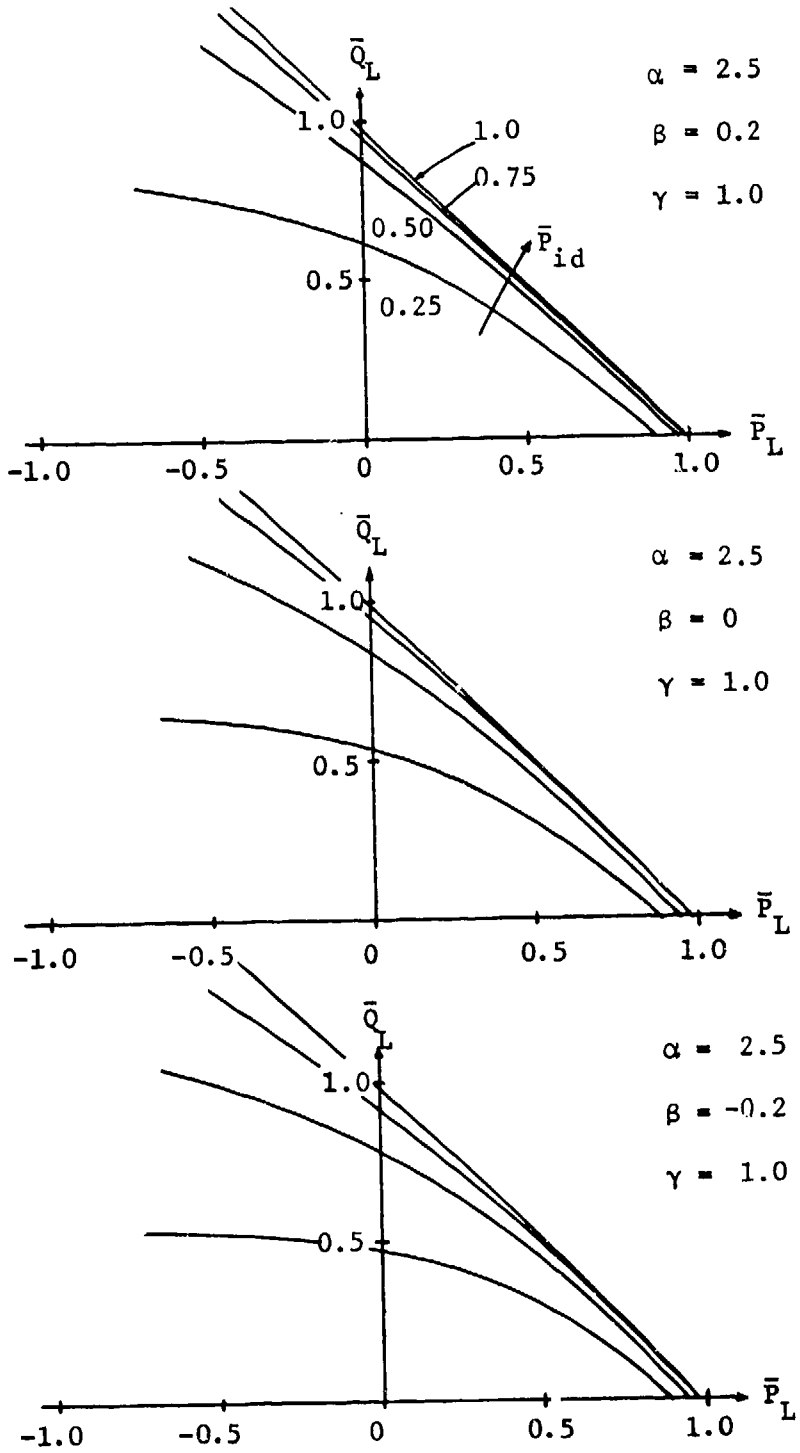

Figure 9. Servovalve characteristics for values of α, β and γ

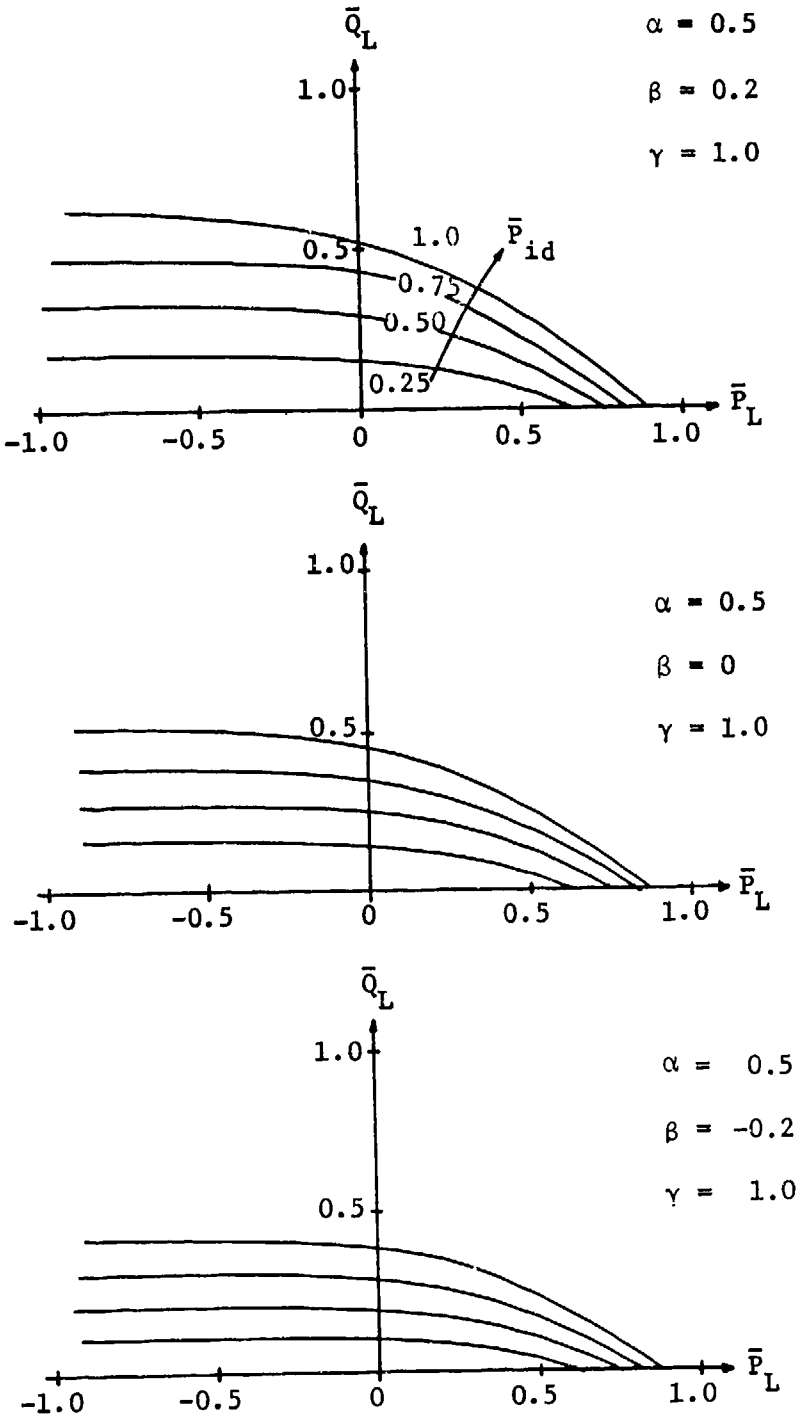

Figure 9. Servovalve characteristics for values of α, β and γ. (con'd)

control valve or to have a blend of pressure/flow control characteristics. Thus, the valve may be specifically designed for matching a given load.

2.4 Component Selection

The three quantities α, β and γ completely characterize the nondimensional output pressure/flow characteristics of the general valve configuration. The values of the valve feedback resistances can be selected to achieve the desired values of α, β and γ. While α, β and γ can be selected independently, the resistances are interrelated and are also dependent upon amplifier parameters.

If it is assumed that a basic multistage gain block has been constructed to provide the maximum required levels of absolute pressure and flow, then the amplifier values of K_p, K_q, P_{cds}, Q_{Ls}, P_{Ls} and R_a are known. When these values are coupled with a set of desired values of α, β and γ selected to yield the overall valve characteristics, the following method may be used to select dimensional values of feedback resistances.

The value of α may be written as

$$\alpha = \frac{R'}{R_i} K_p \frac{P_{idm}}{P_{Lm}} \approx \frac{R_a}{R_a + R_i} K_p \frac{P_{idm}}{P_{Lm}} \qquad (18)$$

where it is noted that because R_a and R_i are usually small compared with other resistances R'/R_i is approximated by $R_a/(R_a + R_i)$. Thus from α and amplifier parameters, R_i and the approximation to R' may be determined when a maximum control input pressure differential P_{idm} is selected. Once R' is calculated then R_{fp} may be determined directly from the requirement to match γ in equation (11). The resistance R_{fq} is determined from the requirement to match β in equation (10) after the flow sensing resistor R_Q has been determined.

The flow sensing resistor R_Q is selected to provide a low resistance so that the flow is not restricted through the load and provide a sufficiently large resistance so that a reasonable value of R_{fq} is obtained for the given value of β. If R_{fq} is too small then the amplifier output is loaded down and large feedback flows occur.

Based upon the detailed development of valve design procedures,[7] a good guideline for R_Q is given by

$$\frac{0.2}{K_{qp}} < R_Q < \frac{0.4}{K_{qp}} \tag{19}$$

Once R_Q is selected all other design resistance values may be directly computed.

2.5 Small Perturbation Characteristics

The static characteristics of the servovalve for incremental deviations from an operating point may be derived by linearizing the nonlinear static characteristic. The result of linearizing equation (12) is

$$\bar{Q}_L = \frac{1}{(1-\beta)} [\alpha \Delta \bar{P}_{id} + (\gamma - 1)\Delta \bar{P}_L] \tag{20}$$

where $\Delta(\ )$ indicates an incremental deviation.

The servovalve flow gain G_q and pressure gain G_p derived from equation (20) are

$$G_p = \left.\frac{\partial P_L}{\partial P_{id}}\right|_{Q_L=0} = \frac{1}{R_i} \frac{K_p R'}{1 - \frac{K_p R'}{R_{fp}}} \tag{21}$$

$$G_q = \left.\frac{\partial Q_L}{\partial P_{id}}\right|_{P_L=0} = \frac{1}{R_i} \frac{1}{1 + K_q R'\left(\frac{1}{R_{fq}} - \frac{1}{R_{fp}} + \frac{1}{K_p R'}\right)} \tag{22}$$

---

[7] D. Lee, The Analytical and Experimental Development of a Fluidic Servovalve, Massachusetts Institute of Technology, Ph.D Thesis (April 1980).

The valve blocked load pressure gain and no load flow gain are expressed in equations (21) and (22) directly in terms of feedback element and amplifier parameters. The pressure gain can be maximized by setting $R_{fp} = K_p R'$ which is equivalent to setting $\gamma = 1$. If this condition is met the pressure gain approaches infinity and the output curves approach horizontal lines in Figure 9 indicating a load insensitivity. The blocked load pressure gain is sensitivity to R_{fp}. For large R_{fp} the positive pressure feedback is small and G_p/K_p approaches $R_a/(R_a + R_i)$ and for small values of R_{fp}, G_p/K_p increases markedly as R_{fp} is reduced.

The flow gain given in equation (22) decreases as R_{fp} is reduced and increases as R_{fp} is reduced.

Both the valve pressure gain G_p and flow gain G_q are functions of the amplifier pressure gain K_p and flow gain K_q. Because of the servovalve positive pressure and negative flow feedback, the servovalve pressure gain increases faster than the amplifier pressure gain while the servovalve flow gain increases less rapidly than the amplifier flow gain.

3. PROTOTYPE SERVOVALVE CONSTRUCTION AND EVALUATION

3.1 Servovalve Construction

The general relationships derived in the previous section have been used to design two prototype servovalve configurations. Both prototype servovalves have been constructed by using the three stage gain amplifier summarized in Table 1 and laminar flow resistors constructed from small cross section rectangular passages. The servovalve's general configuration is illustrated in Figure 10. The basic three-stage amplifier is shown with the stages stacked back to back, separated by manifold plates. The pressure and flow feedbacks as well as the flow sensing resistors are connected directly to the output ports of the final amplifier stage through a manifold. The low pressure sides of the feedback resistors are connected to the control ports of the amplifier first stage through flexible plastic hoses. Vent ports labeled V_1, V_2 and V_3 are piped to the reservoir. A flapper nozzle valve driven by a torque motor

TABLE 1: FLUIDIC AMPLIFIER CONFIGURATION

A. LAMINATE DESCRIPTION

Parameter	Value
Design	HDL 3.1.1.8
Laminate Height	h_s = 0.1 mm [0.004 in.]
Supply Nozzle Width	b_s = 0.5 mm [0.020 in.]

B. THREE-STAGE AMPLIFIER

Stage	Section aspect ratio, ($\sigma = h_s/b_s$)	Number of sections per amplifier	Supply pressure, P_s (kPa) [psi]	Estimated supply flow Q_s (m^3/s) [cis]
1	0.6	2	620 [90]	0.70×10^{-5} [0.43]
2	0.6	3	2068 [300]	1.9×10^{-5} [1.18]
3	0.4	4	6895 [1000]	3.1×10^{-5} [1.91]

C. AMPLIFIER INCREMENTAL PARAMETERS

Parameter	Value
P_{ods}	3654 kPa [530 psid]
Q_{Ls}	1.80×10^{-5} m^3 [1.1 cis]
P_{cds}	9.96 kPa [1.45 psid]
K_p	367
K_q	1.805×10^{-6} $m^3/s/kPa$ [0.76 cis/psid]
K_{qp}	4.99×10^{-9} $m^3/s/kPa$ [0.0021 cis/psid]

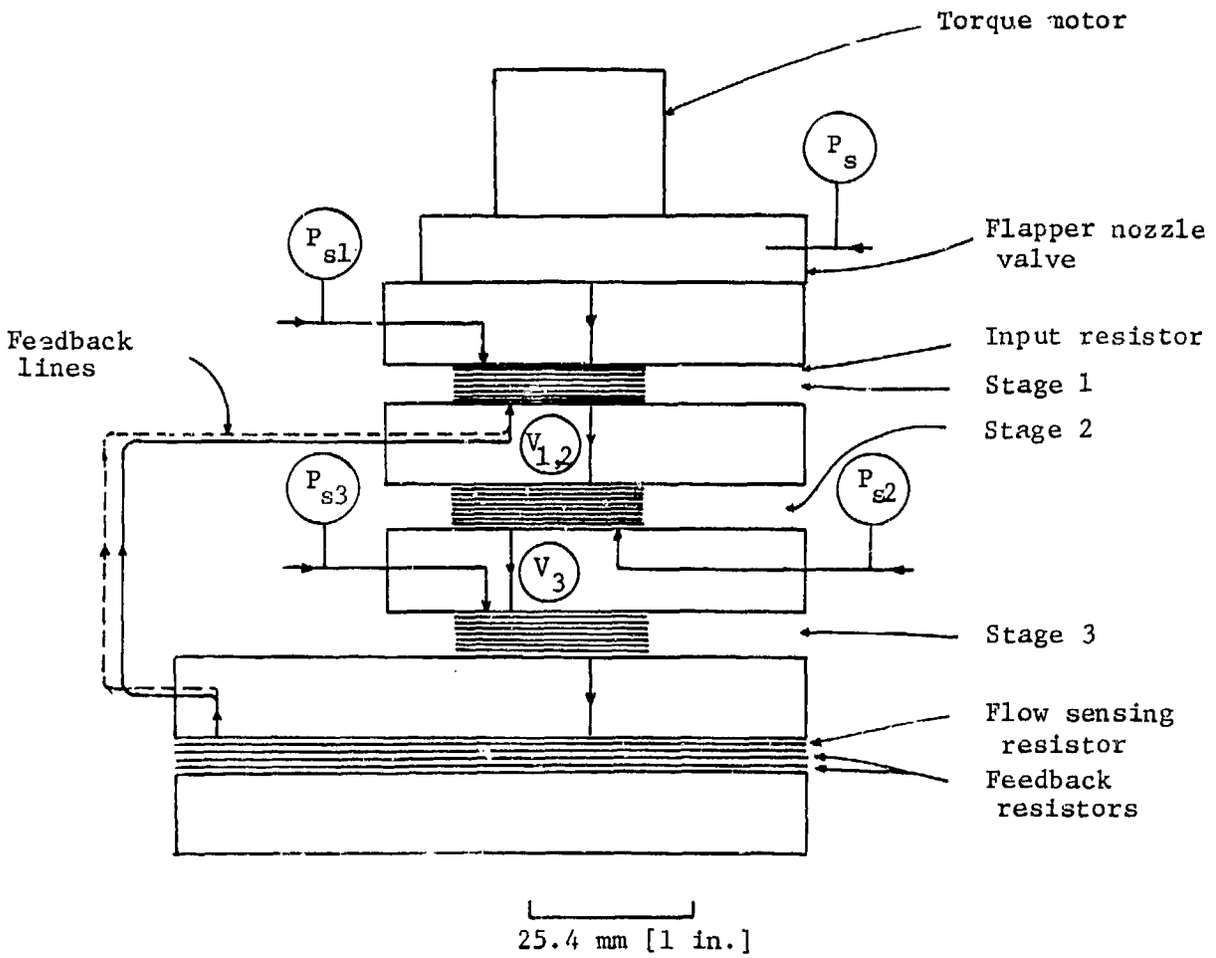

Figure 10 Schematic of servovalve design.

is used as an input signal generator to the servovalve. It is connected to the servovalve through the input resistor R_i.

The general servovalve configuration is a breadboard configuration that permits measurement of pressures at each stage in the amplifier and feedback network. It has been constructed by using HDL 3.1.1.8 laminates. However, the overall configuration has not utilized the standard packaging techniques which allow an integrated package to be constructed since it was desired to make measurements in the servovalve at many intermediate locations.

In all tests performed on the servovalves, Univis J-43 oil maintained at an operating temperature of 27°C was used. Under this condition the fluid density is 8.69×10^2 N-s^2/m^4 and the viscosity is 1.88×10^{-2} N-s/m^2.

Two servovalves have been constructed and tested. The two valves are similar except for the values of feedback resistors. Servovalve 1 was constructed with $\alpha = 1.2$, $\beta = 0$ and $\gamma = 1$ while servovalve 2 was constructed with $\alpha = 1.2$, $\beta = -0.2$ and $\gamma = 1$.

3.2 Resistor Characteristics

Laminar flow resistors made from small cross section area rectangular ducts are used in the servovalve. The resistors were made by cutting a slot in brass shim stock and sandwiching the shim stock between two manifold plates. This type of resistor is simple to construct and is self-bleeding, i.e., air bubbles are forced out of the passageway with the oil flow. An example resistor is shown in Figure 11. The shim resistor includes serveral holes for mounting, alignment and porting. The thickness of the shim, the width of the milled slot and the length of the slot determine the resistance as well as the viscosity of the fluid.

The dimensions and resistance values of the resistors used in the servovalves are summarized in Table 2. The measured pressure-flow characteristics of the feedback and input resistors are shown in Figure 12. They are linear over the range of the test.

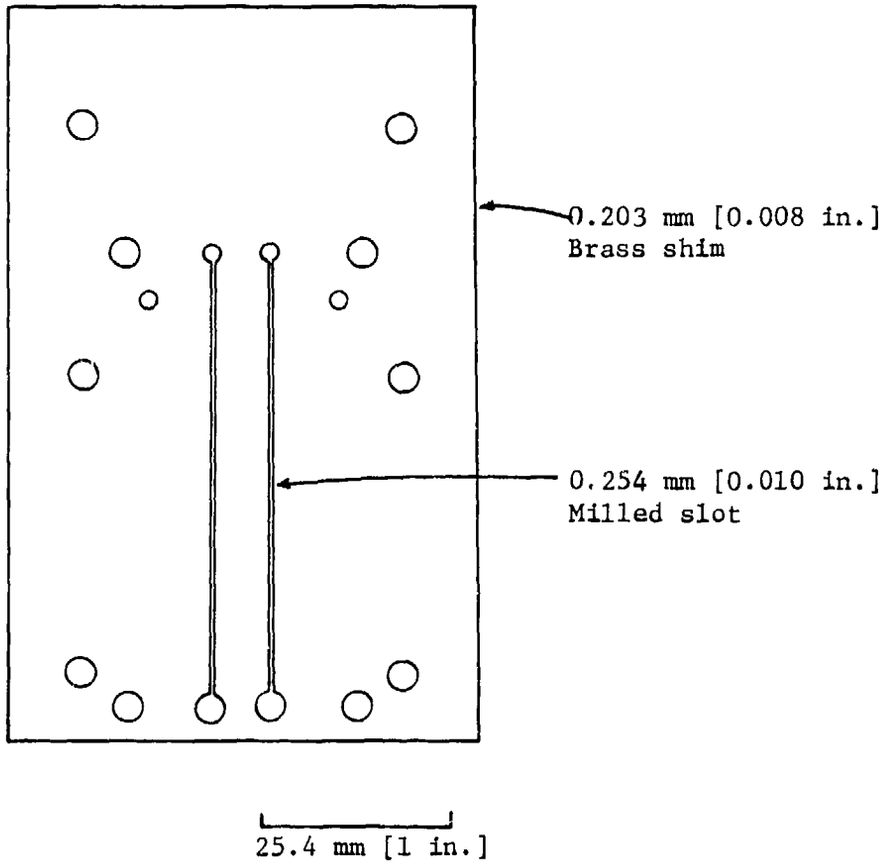

Figure 11. Pressure feedback resistor design.

TABLE 2: RESISTOR DIMENSIONS AND VALUES

Resistor	Width [mm]	Height [mm]	Length [mm]	Measured resistance $N\text{-}s/m^5$	Estimated inertance $N\text{-}s^2/m^5$
R_i	0.533	0.813	12.7	2.48×10^{10}	2.53×10^{7}
R_i	0.304	0.813	8.89	5.30×10^{10}	3.07×10^{7}
R_Q	3.175	0.406	27.94	3.83×10^{10}	1.85×10^{7}
R_Q	6.35	0.203	27.94	9.30×10^{10}	1.85×10^{7}
R_{fp}	0.254	0.203	57.15	7.22×10^{12}	9.56×10^{8}
R_{fp}	0.203	0.203	57.15	1.20×10^{13}	1.19×10^{9}
R_{fp}	0.254	0.203	57.15	7.22×10^{12}	9.56×10^{8}

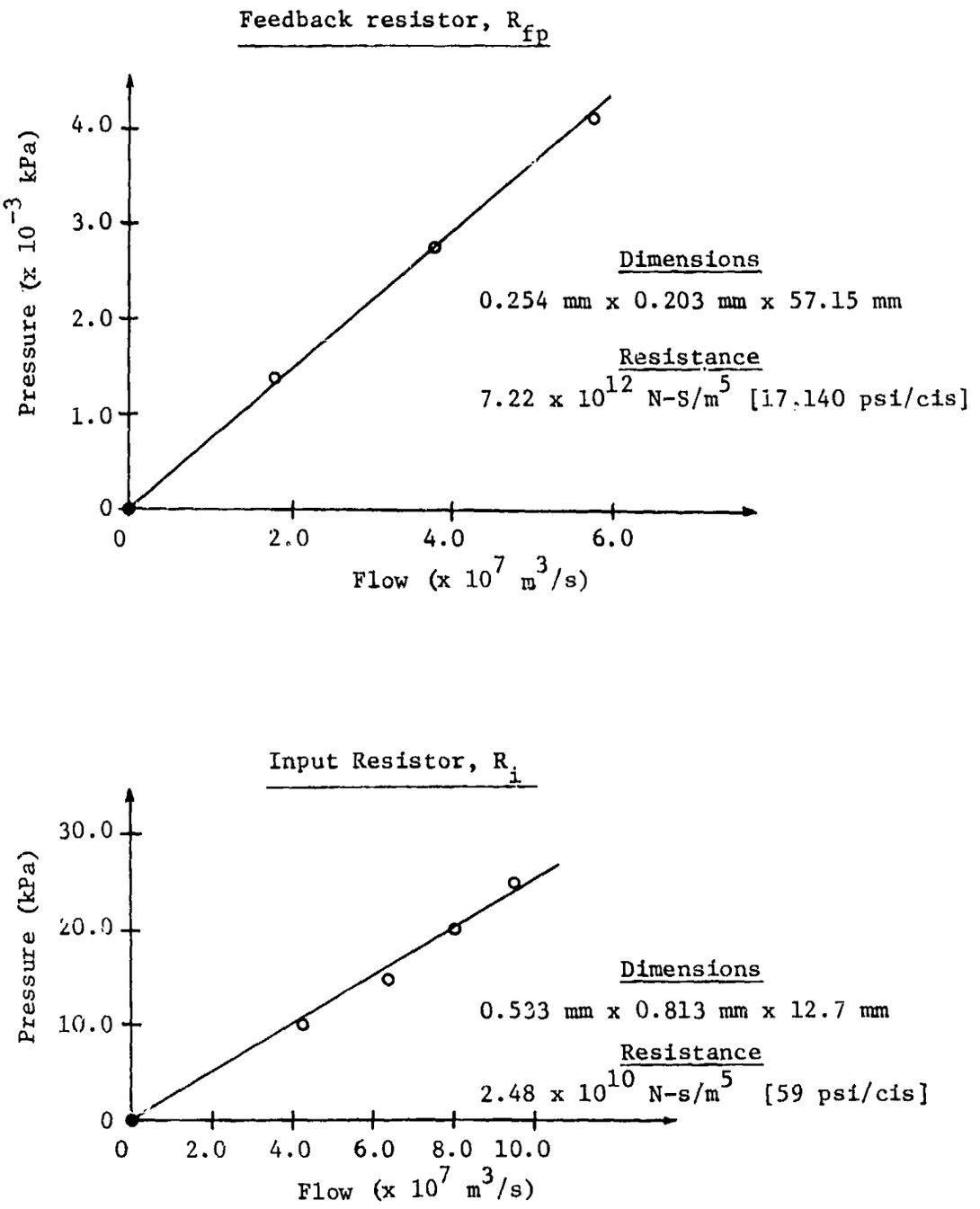

Figure 12. Resistor characteristics.

3.3 Multistage Amplifier Characteristics

A summary of the multistage amplifier parameters is given in Table 1. The three stage amplifier output pressure/flow characteristics are presented in Figure 4, where they have been compared with the analytical expression of equation (12). As noted in Section 2, the analytical expression agrees well with the data. As shown by the data the multistage amplifier has good saturation characteristics and an input pressure of about 10 kPa produces a saturation output pressure of 3650 kPa.

3.4 Servovalve Static Characteristics

Two servovalve configurations have been constructed and tested. The two valves both consist of the multistage gain amplifier described in the previous section and the laminar flow resistors. The parameters for the two servovalve configurations are summarized in Table 3.

The static characteristics of the two configurations have been measured in all four quadrants of operation using the experimental techniques described by Lee.[7] The experimental data are displayed in Figures 13 and 14 and are compared with the analytically predicted characteristics. The experimental data for both servovalve configurations agree closely with the theoretical data. Some asymmetry is illustrated in the experimental characteristics which is due to asymmetry in the multistage amplifier characteristics. It is expected that these asymmetries can be eliminated when the multistage amplifier is fabricated with more uniform manufacturing methods rather than built up in a breadboard configuration.

The differences between the two valve configurations due to the values of the flow coefficient β are reflected in both the experimental and theoretical data. Configuration 1 ($\beta = 0$) has load pressure/flow characteristics which have a significant slope and represent a blend of pressure/flow control characteristics. Configuration 2 ($\beta = -0.21$) has load pressure/flow characteristics that are relatively flat indicating a low sensitivity to load

[7] D. Lee, The Analytical and Experimental Development of a Fluidic Servovalve, Massachusetts Institute of Technology, Ph.D. Thesis (April 1980).

TABLE 3: SERVOVALVE CONFIGURATIONS

Parameter	Parameter Value	Parameter Value
	Configuration 1	Configuration 2
α	1.24	1.24
β	0	-0.21
γ	0.99	1.0
R_i	2.48×10^{10} N-s/m^5	5.3×10^{10} N-s/m^3
R_Q	3.83×10^{10} N-s/m^5	9.3×10^{10} N-s/m^3
R_{fp}	7.22×10^{12} N-s/m^5	1.2×10^{13} N-s/m^3
R_{fq}	7.22×10^{12} N-s/m^5	7.22×10^{12} N-s/m^3
R_a	8.55×10^{10} N-s/m^5	8.55×10^{10} N-s/m^3
P_{Lm}	3654 kPa	3654 kPa
Q_{Lm}	1.51×10^{-5} m^3/s	1.22×10^{-5} m^3/s

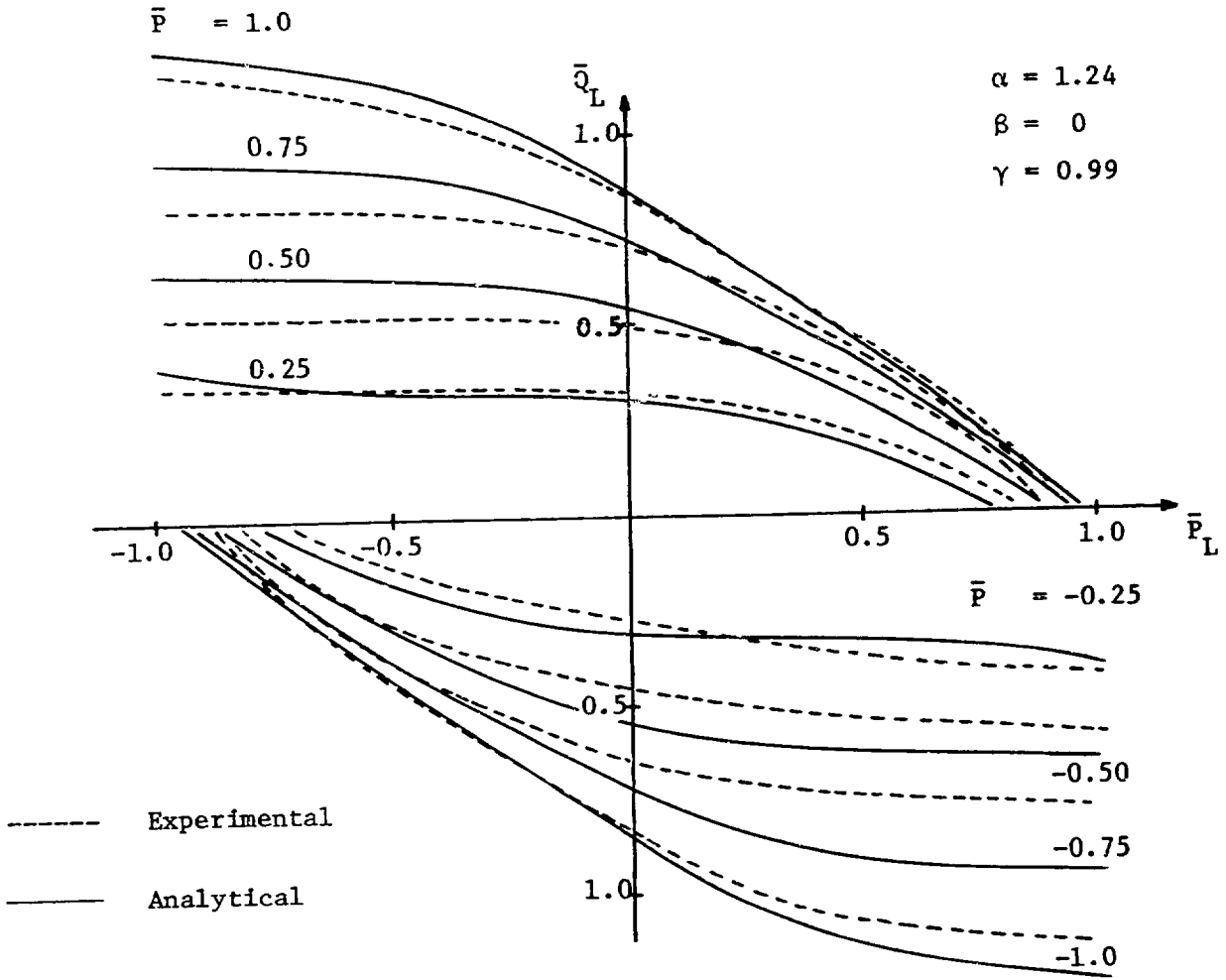

Figure 13. Configuration 1 servovalve output characteristics.

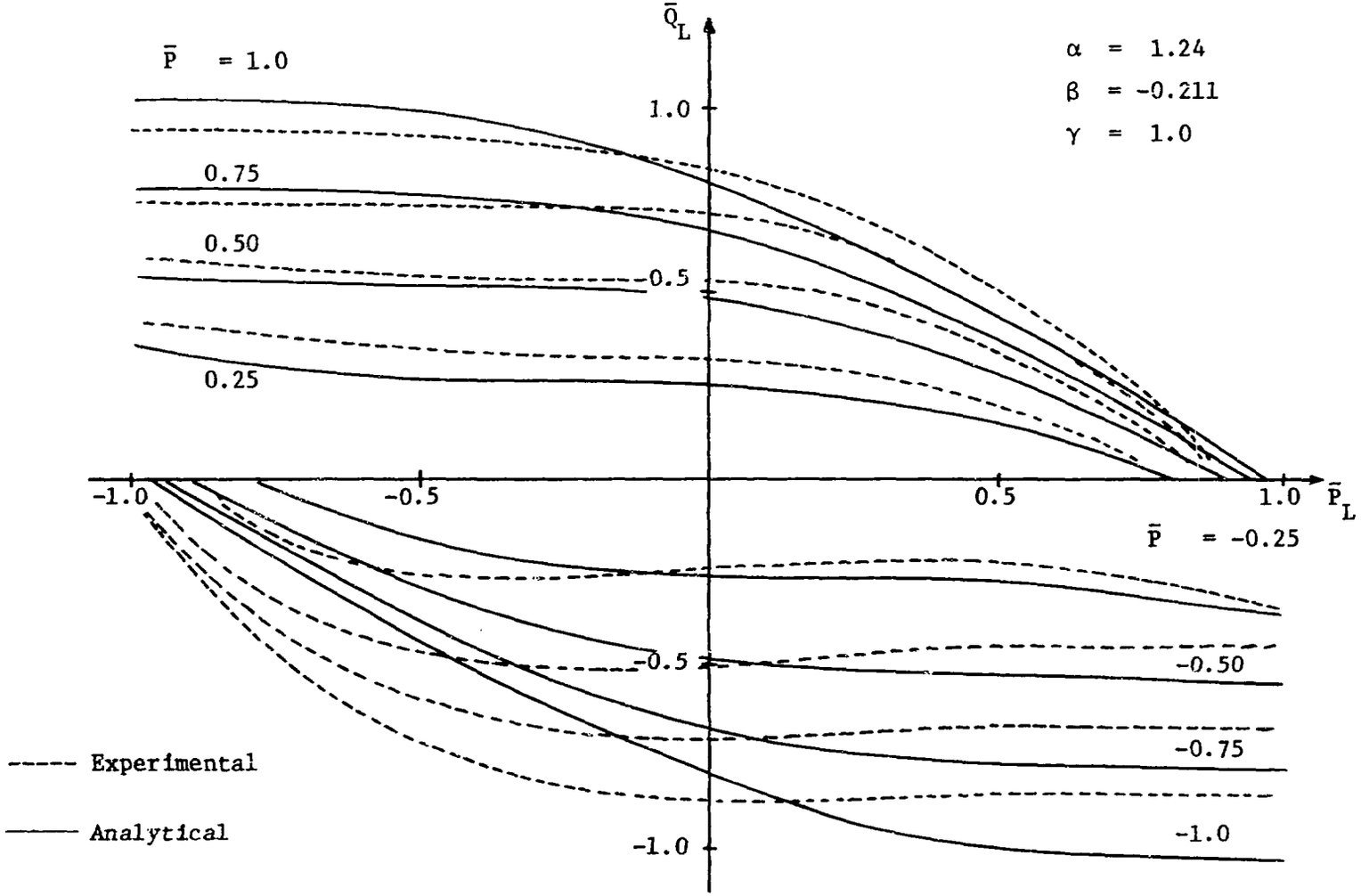

Figure 14. Configuration 2 servovalve output characteristics.

pressure. The output characteristic of configuration 1 is similar to that of the spool valve shown in Figure 1 while the output characteristics of configuration 2 are less sensitive to load pressure than those of a spool valve. The data show that as β is decreased the curves approach an ideal flow control valve in which the output flow is insensitive to load pressure.

3.5 Servovalve Efficiency and Quiescent Flow

Measures of servovalve effectiveness include the fraction of total valve power delivered to a load and the quiescent flow drain. The normalized efficiency, η, of the fluidic servovalve can be defined as the power delivered to the load divided by the maximum load pressure/load flow product:

$$\eta = \frac{P_L Q_L}{P_{Lm} Q_{Lm}} \tag{23}$$

This measure of efficiency is plotted in Figure 15 for comparison with the efficiency of a spool valve defined as

$$\eta = \frac{P_L}{P_s}\sqrt{1 - \frac{P_L}{P_s}} \tag{24}$$

and double flapper nozzle valve with equal upstream and downstream orifices where the efficiency is defined

$$\eta = \frac{P_L Q_L}{P_{Lm} Q_{Lm}} \tag{25}$$

The figure indicates that all three valves reach peak efficiencies with $0.51 < P_L/P_{Lm} < 0.7$ with the spool valve maximum of 0.38, the flapper nozzle valve of maximum 0.33 and the fluidic valve maximum of 0.27. This comparison shows that the fluidic valve power ratio is 70% of the spool valve and 82% of the double flapper nozzle valve.

In addition to the power ratio, the quiescent flow through the valve is of interest. The spool valve is a closed center valve and ideally the spool has 0% leakage while in practice spool leakage rates are often 5 to 10% of the spool maximum flow. The double flapper nozzle valve and the

Valve	Efficiency, η	Description
Spool	$\frac{P_L Q_L}{P_s Q_{Lm}}$	Closed center
Flapper nozzle	$\frac{P_L Q_L}{P_{Lm} Q_{Lm}}$	Equal null upstream and downstream orifice areas
Fluidic	$\frac{P_L Q_L}{P_{Lm} Q_{Lm}}$	$\alpha = 1.2$ $\beta = -0.2$ $\gamma = 1.0$

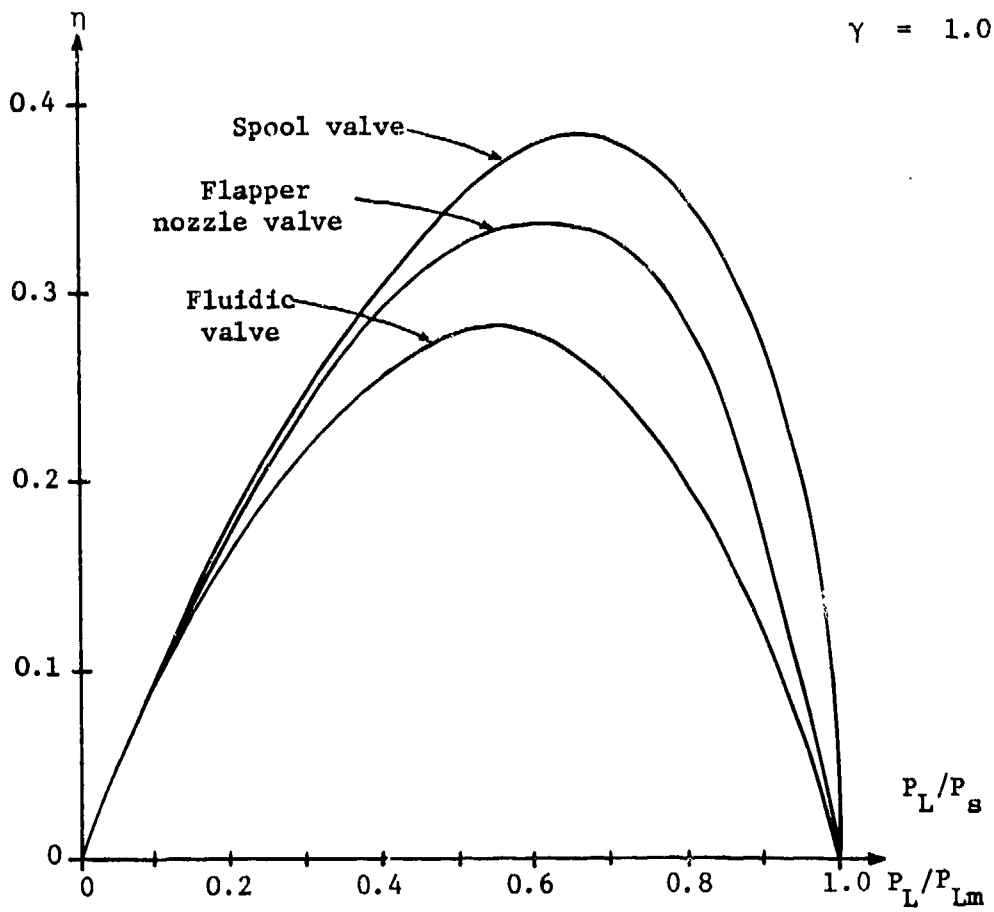

Figure 15. Servovalve efficiencies.

fluidic valve are both open center valves. The flapper nozzle valve has a maximum load flow to quiescent flow ratio of 1 while the fluidic servovalve has a ratio of 0.31.

In the fluid servovalve, the maximum flow delivered to the load is 1.8×10^{-5} m^3/s while the quiescent flow in the three stages of the amplifier is 5.76×10^{-5} m^3/s. It is anticipated that through modification of the multistage amplifier design the ratio of load to quiescent flow may be increased significantly.

4. SERVOVALVE DYNAMIC PERFORMANCE

4.1 Dynamic Model

A dynamic model for the servovalve valid for small perturbations from an operating point may be synthesized from models for the multistage amplifier and the circuit resistors.

The circuit input and feedback resistors are constructed from laminar flow passages which have a measurable inertance as well as resistance. Dynamically each resistor is represented as an impedance:

$$Z_j(s) = R_j + L_j s \tag{26}$$

where

Z_j = impedance of element j
R_j = resistance of element j
L_j = jth fluid inertance
s = Laplace operator

The value of each R_j is taken from the experimental measurements cited in Section 3 while the inertance is estimated from the relationship

$$L_j = \rho \frac{\ell_j}{A_j} \tag{27}$$

where

ρ = fluid density
ℓ_j = jth passage length
A_j = jth passage area

The values of inertance for each resistor are listed in Table 2.

The multistage amplifier for incremental deviations may be represented as a dynamic pressure and flow gain:

$$\frac{\Delta P_{od}(s)}{\Delta P_{cd}(s)} = H_p(s) \tag{28}$$

$$\frac{\Delta Q_L(s)}{\Delta P_{cd}(s)} = H_q(s) \tag{29}$$

where

$H_p(s)$ = amplifier dynamic pressure gain transfer function

$H_q(s)$ = amplifier dynamic flow gain transfer function

Studies by Lee[7] have shown that the two amplifier transfer functions may be represented as

$$H_p = K_p \frac{1 - (T_p/2)s + (T_p^2/8)s^2}{1 + (T_p/2)s + (T_p^2/8)s^2} \tag{30}$$

$$H_q = K_q \frac{1 - (T_q/2)s + (T_q^2/8)s^2}{1 + (T_q/2)s + (T_q^2/8)s^2} \tag{31}$$

where

T_p = amplifier pressure gain delay time

T_q = amplifier flow gain delay time

The amplifier pressure and flow gain transfer functions given in

[7] D. Lee, The Analytical and Experimental Development of a Fluidic Servovalve, Massachusetts Institute of Technology, Ph.D. Thesis (April 1980).

equations (30) and (31) are compared in Figures 16 and 17 with experimentally measured amplifier characteristics for $T_p = 1.1 \times 10^{-3}$ s and $T_q = 1.1 \times 10^{-3}$ s. There is close agreement between the experimental data and the analytical expressions.

The complete servovalve dynamic transfer function for small deviations may be derived replacing the static gains and resistances in equations (21) and (22) with the dynamic equivalents to obtain

$$G_p(s) = \frac{1}{Z_i(s)} \quad \frac{H_p(s)Z'(s)}{1 - \frac{1}{Z_{fp}(s)} H_p(s)Z'(s)} \tag{32}$$

$$G_q(s) = \frac{1}{Z_i(s)} \frac{H_q(s)Z'(s)}{1 + H_q(s)Z'(s)Z_Q(s)\left[\frac{1}{Z_{fq}(s)} - \frac{1}{Z_{fp}(s)} + \frac{1}{H_p(s)Z'(s)}\right]} \tag{33}$$

These two expressions provide an analytical representation of the servovalve dynamic pressure and flow gain responses.

4.2 Experimental Dynamic Performance

The dynamic frequency response characteristics of the servovalve have been measured by using the techniques described by Lee.[7] The experimentally measured pressure and flow gains as a function of frequency are plotted in Figures 16 and 17 for valve configuration 1. The data show that the pressure gain reaches 90 deg phase shift at 7 Hz and the flow gain reaches 90 deg phase shift at approximately 60 Hz.

The analytical expressions given in equations (32) and (33) also are plotted. In the analysis the impedances are represented by the values of resistance and inertance cited in Table 2. However, for cases in which

[7] D. Lee, The Analytical and Experimental Development of a Fluidic Servovalve, Massachusetts Institute of Technology, Ph.D. Thesis (April 1980).

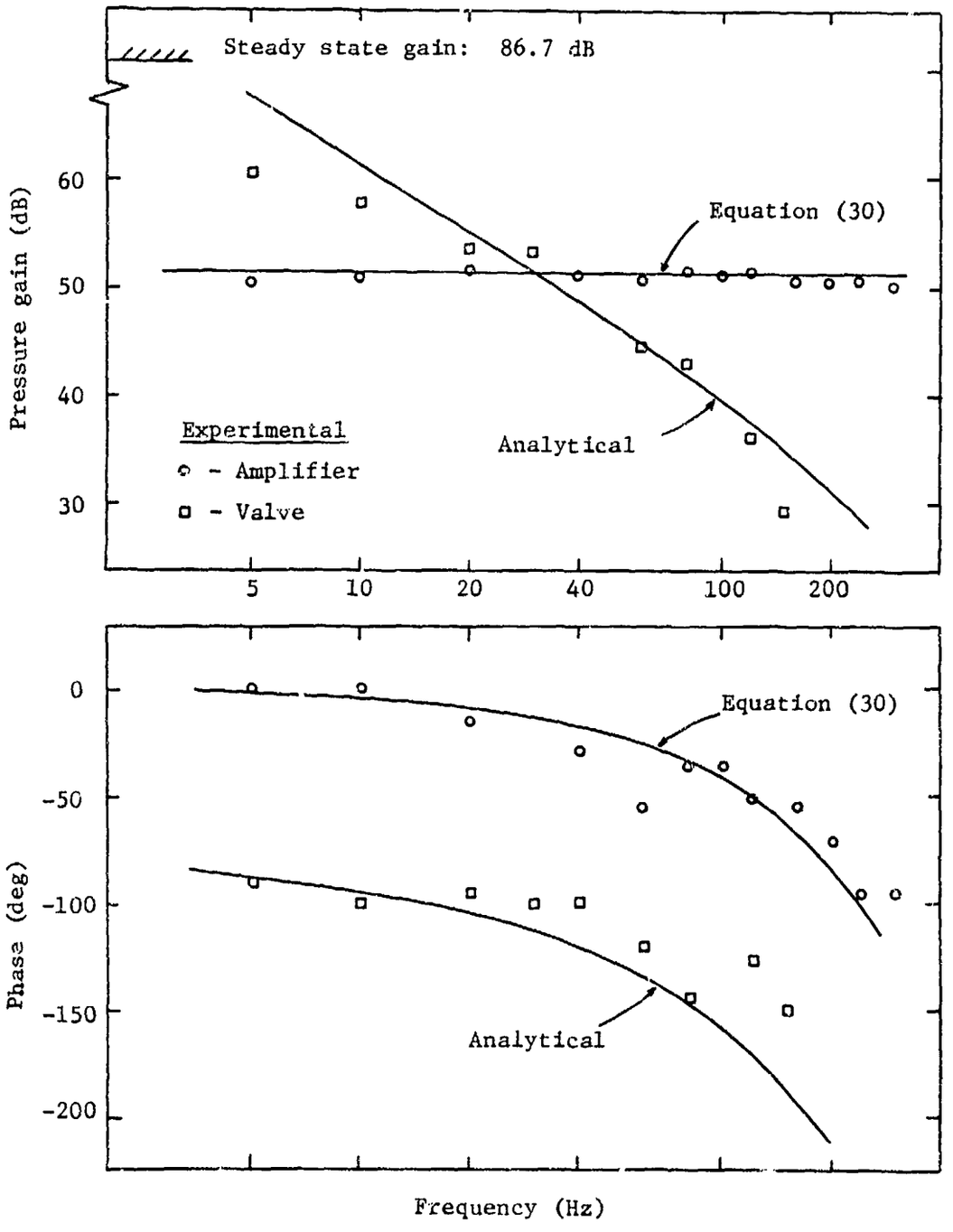

Figure 16. Amplifier and servovalve blocked load frequency response.

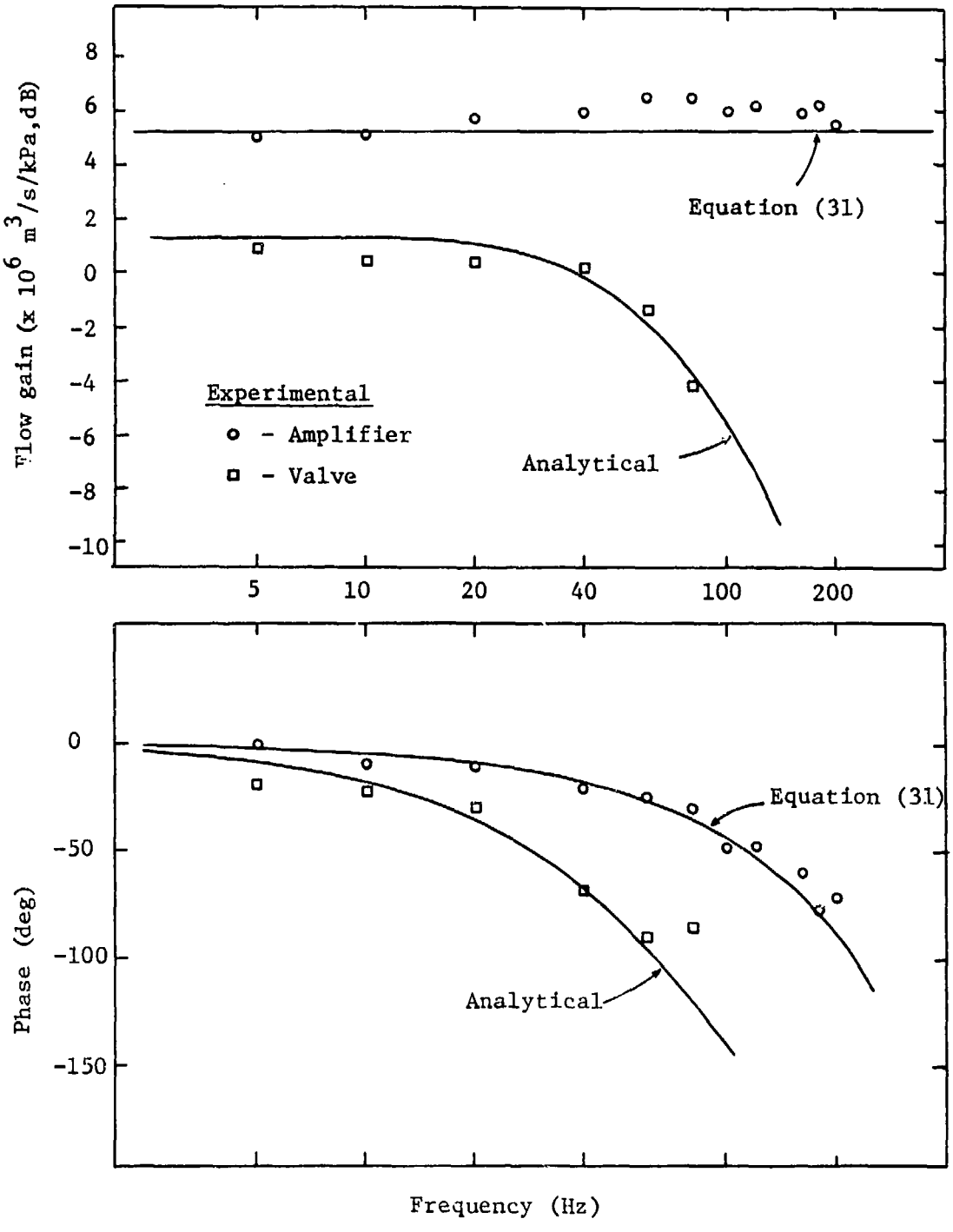

Figure 17. Amplifier and servovalve no load frequency response.

$L_j/R_j < 1.6 \times 10^{-4}$ s, the inertance L_j was neglected since it represents less than 10% of the impedance at frequencies below 100 Hz. Also the impedance for the resistor R_a was modified to include the capacitance in the flexible plastic hoses. Thus, the impedance Z_a was represented with inertance neglected and hose capacitance included as

$$Z_a = \frac{R_a}{R_a Cs + 1} \tag{34}$$

where

$C = 171\ m^5/N$ as determined by Lee.[7]

The dynamic model including the effects of hose capacitance agrees closely with the experimental data.

In the valve tested, the use of the flexible feedback hoses contribute to the valve dynamic response. If the hose capacitance is eliminated, the analytical model indicates that the flow gain frequency response can be extended beyond 100 Hz before 90 deg phase shift occurs while the pressure gain frequency response is extended beyond 20 Hz at 90 deg phase shift.

It is anticipated that construction of the servovalve in an integrated package would extend the flow gain frequency response into the 100 Hz range before 90 deg phase shift is reached.

In commercial electrohydraulic servovalves of the same flow capability as the fluidic servovalve, the flow gain frequency response has been measured which indicates the 90 deg phase shift is reached at about 100 Hz.[6]

---

[6] D. Lee and D. N. Wormley, Multistage Hydraulic Summing and Signal Processing Amplifiers and Fluidic Input Servovalve Development, Harry Diamond Laboratories, HDL-CR-76-233-1 (1976).

[7] D. Lee, The Analytical and Experimental Development of a Fluidic Servovalve, Massachusetts Institute of Technology, Ph.D. Thesis (April 1980).

SUMMARY AND CONCLUSIONS

A pure fluid servovalve configuration has been developed which has output pressure/flow characteristics that can be contoured to be similar to flow or pressure control servovalves or a blend of these characteristics. General static design relationships have been derived for configurations employing multistage fluid amplifiers and linear resistance elements. The relationships are useful in determining the feedback element parameters required to achieve a specified output characteristic.

Two prototype valve configurations were constructed by using standard laminar proportional amplifiers. The data obtained with these valves verifies the general static and dynamic analyses. It has demonstrated the ability to contour static characteristics through changes in feedback elements and indicated a dynamic flow response potential which is comparable to commercial electrohydraulic valves of the same flow capability. The valve configurations tested were constructed in breadboard fashion and thus both improvements in dynamic response and reduction in overall size is possible when integrated circuit designs are employed.

The study has identified several areas for further development. To achieve a minimum size and weight valve with standard components, servovalves should be constructed with HDL standard integrated laminates, spacers and resistors in an integrated package. A preliminary layout study has shown that construction of a valve similar to configuration 1 with the standard elements is possible in a package approximately 3 x 3 x 5 cm which weighs 0.65 kg. Thus, fluid servovalves have potential for reduced size and weight in comparison to typical spool valves of the same capability.

In the current study, the servovalves were evaluated with hydraulic oil maintained at ambient temperature. Further effort is planned to evaluate valve performance as a function of temperature.

One of the attributes of the pure fluidic valve is the relatively high quiescent flow requirement associated with open center valves. Further optimization of the multistage gain amplifier is merited to reduce the ratio of the quiescent to maximum load flow.

NOMENCLATURE

A_j	jth passage area
b_s	supply nozzle width (figure 2)
C	fluid capacitance
G_p	servovalve pressure gain
G_q	servovalve flow gain
H_p	amplifier dynamic pressure gain
H_q	amplifier dynamic flow gain
K_p	incremental amplifier static pressure gain
K_q	incremental amplifier static flow gain
K_{qp}	incremental amplifier output admittance (equation 5)
ℓ_j	jth passage length
L	load (figure 5)
L_j	jth fluid inertance
P_{cd}	amplifier input pressure differential
P_{cds}	amplifier saturation input differential
$P_{c\ell}$	amplifier left input pressure (figure 3)
P_{cr}	amplifier right input pressure (figure 3)
P_{id}	servovalve input pressure differential
P_{idm}	maximum servovalve input pressure differential
$P_{i\ell}$	servovalve left input pressure (figure 5)
P_{ir}	servovalve right input pressure (figure 5)
P_L	pressure drop across load (equation 8)
P_{Lm}	maximum pressure drop across load (equation 11)
P_{od}	amplifier output pressure differential
P_{ods}	saturation amplifier output pressure differential
$P_{o\ell}$	pressure defined in figures 3 and 6
$P_{o\ell'}$	pressure defined in figure 6
P_{or}	pressure defined in figures 3 and 6
P_s	supply pressure
P_1	pressure defined in figure 1

P_2	pressure defined in figure 1
Q_L	output load flow
Q_{Ls}	saturation output load flow
Q_{Lm}	maximum output load flow (equation 10)
Q_s	supply flow
R_a	amplifier control port input resistance
R_{fp}	pressure feedback resistance
R_{fq}	flow feedback resistance
R_i	servovalve input resistance
R_Q	flow sensing resistor
R'	parallel combination of R_i, R_a, R_{fq}, R_{fp}
S	Laplace Operator
T_p	amplifier pressure gain delay time
T_q	amplifier flow gain delay time
V	vent (figure 10)
x	valve spool displacement (figure 1a)
Z_a	impedance defined in equation 34
Z_{fp}	pressure feedback impedance
Z_{fq}	flow feedback impedance
Z_i	servovalve input impedance
Z_j	impedance of element j
Z_a	flow sensing impedance
Z'	parallel combination of Z_i, Z_a, Z_{fp}, Z_{fq}
α	nondimensional valve coefficient (equation 13)
β	nondimensional valve coefficient (equation 14)
γ	nondimensional valve coefficient (equation 15)
η	efficiency
ρ	fluid density

DISTRIBUTION

ADMINISTRATOR
DEFENSE TECHNICAL INFORMATION CENTER
ATTN DTIC-DDA (12 COPIES)
CAMERON STATION, BUILDING 5
ALEXANDRIA, VA 22314

COMMANDER
US ARMY RSCH & STD GP (EUR)
ATTN CHIEF, PHYSICS & MATH BRANCH
FPO NEW YORK 09510

COMMANDER
US ARMY MATERIAL DEVELOPMENT &
READINESS COMMAND
ATTN DRCLDC, MR. J. BENDER
5001 EISENHOWER AVENUE
ALEXANDRIA, VA 22333

COMMANDER
US ARMY ARMAMENT MATERIAL
READINESS COMMAND
ATTN DRSAR-ASF, FUZE &
MUNITIONS SUPPORT DIV
ATTN DRSAR-RDF, SYS DEV DIV-FUZES
ATTN DRSAR-RDG-T, R. SPENCER
ATTN DRSAR-ASF
ATTN DRSAR-LEP-L, TECH LIBRARY
ROCK ISLAND, IL 61299

COMMANDER
US ARMY MISSILE & MUNITIONS
CENTER & SCHOOL
ATTN ATSK-CTD-F
REDSTONE ARSENAL, AL 35809

DIRECTOR
US ARMY MATERIAL SYSTEMS
ANALYSIS ACTIVITY
ATTN DRXSY-MP
ABERDEEN PROVING GROUND, MD 21005

DIRECTOR
US ARMY BALLISTIC RESEARCH LABORATORY
ATTN DRDAR-TSB-S (STINFO)
ABERDEEN PROVING GROUND, MD 21005

US ARMY ELECTRONICS TECHNOLOGY
AND DEVICES LABORATORY
ATTN DELET-DD
FORT MONMOUTH, JN 07703

HQ, USAF/SAMI
WASHINGTON, DC 20330

TELEDYNE BROWN ENGINEERING
CUMMINGS RESEARCH PARK
ATTN MELVIN L. PRICE, MS-44
HUNTSVILLE, AL 35807

COMMANDER IDDR&E
PENTAGON, ROOM 3D 1089
ATTN G. KOPCSAK
WASHINGTON, DC 20310

OFFICE OF THE DEPUTY CHIEF OF STAFF FOR
RESEARCH, DEVELOPMENT & ACQUISITION
DEPARTMENT OF THE ARMY
ATTN DAMA-ARP-P
ATTN DAMA-CSS
WASHINGTON, DC 20310

US ARMY R&D GROUP (EUROPE)
BOX 15
ATTN CHIEF, AERONAUTICS BRANCH
ATTN CHIEF, ENGINEERING SCIENCES
FPO NEW YROK 09510

US ARMY RESEARCH OFFICE
ATTN R. SINGLETON
P.O. BOX 12211
RESEARCH TRIANGLE PARK, NC 27009

BMD ADVANCED TECHNOLOGY CENTER
ATTN J. PAPADOPOULOS
P.O. BOX 1500
HUNTSVILLE, AL 35807

COMMANDER
US ARMY FOREIGN SCIENCE
& TECHNOLOGY CENTER
FEDERAL OFFICE BUILDING
ATTN DRXST-SD1
ATTN DRXST-IS3, C.R. MOORE
220 7TH STREET, NE
CHARLOTTESVILLE, VA 22901

DIRECTOR
APPLIED TECHNOLOGY LABORATORY
ATTN GEORGE W. FOSDICK, DAVDL-ATL-ASA
FORT EUSTIS, VA 23604

COMMANDER
US ARMY MATERIAL AND MECHANICS
RESEARCH CENTER
ATTN R. KATZ
WATERTOWN, MA 02172

COMMANDER
USA MILLILE COMMAND
ATTN REDSTONE SCIENTIFIC INFORMATION
CENTER, DRSMI-RBD
ATTN DRDMI-TGC, WILLIAM GRIFFITH
ATTN DRDMI-TGC, J.C. DUNAWAY
ATTN DRCPM-TOE, FRED J. CHEPLEN
RESTONE ARSENAL, AL 35809

COMMANDER
US ARMY MOBILITY EQUIPMENT R&D CENTER
ATTN TECHNICAL LIBRARY (VAULT)
ATTN drdme-EM, R. N. WARE
FORT BELVOIR, VA 22060

COMMANDER
EDGEWOOD ARSENAL
ATTN SAREA-MT-T, D. PATTON
ABERDEEN PROVING GROUND, MD 21010

COMMANDER
US ARMY ARRADCOM
ATTN SARPA-TS S #59
ATTN DRDAR-LCN-C, A. E. SCHMIDLIN
ATTN DRDAR-LCW-E, J. CONNORS
ATTN DRDAR-SCF-CC, V. BAUMGARTH
ATTN MICHAEL BACCELLIERI
ATTN PBM-DPM (TAGLAIRINO)
ATTN PBM-MG (A. WILLIAMS)
DOVER, NJ 07801

COMMANDER
WATERVLIET ARSENAL
ATTN SARWV-RDT-L
ATTN DRDAR-LCB-RA, R. RACICOT
WATERVLIET ARSENAL, NY 12189

COMMANDER
US ARMY TANK AUTOMOTIVE R&S &
DEV COMMAND
ARMOR & COMP DIV, DRDTA-RKT
ATTN T. KOZOWYK
ATTN C. DAVIES
BLDG 215
WARREN, MI 48090

COMMANDER
ATTN STEWS-AD-L, TECHNICAL LIBRARY
WHITE SANDS MISSILE RANGE, NM 88002

COMMANDER/DIRECTOR
ATMOSPHERIC SCIENCES LABORATORY
USA ERADCOM
ATTN DELAS-AS (HOLT)
ATTN DELAS-AS-T (R. RUBIO)
WHITE SANDS MISSILE RANGE, NM 88002

OFFICE OF NAVAL RESEARCH
DEPARTMENT OF THE NAVY
ATTN STANLEY W. DOROFF, CODE 438
ATTN D. S. SIEGEL, CODE 211
ARLINGTON, VA 22217

DEPARTMENT OF THE NAVY
R&D PLANS DIVISION
ROOM 5D760, PENTAGON
ATTN BENJ R. PETRIE, JR.
OP-987P4
WASHINGTON, DC 20350

COMMANDANT
US NAVAL POSTGRADUATE SCHOOL
DEPARTMENT OF MECHANICAL ENGINEERING
ATTN CODE 69 Nn(NUNN)
MONTEREY, CA 93940

COMMANDER
NAVAL AIR DEVELOPMENT CENTER
ATTN R. MCGIBONEY, 60134
ATTN CODE 8134, LOIS GUISE
ATTN D. KEYSER, 60134
WARMINSTER, PA 18974

COMMANDER OFFICER
NAVAL AIR ENGINEERING CENTER
ATTN ESSD, CODE 9314, HAROLD OTT
LAKEHURST, NY 08733

NAVAL AIR SYSTEMS COMMAND
DEPARTMENT OF THE NAVY
ATTN CODE AIR-5162C1, J. BURNS
ATTN CODE AIR-5162C8, D. HOUCK
WASHINGTON, DC 20361

COMMANDER
PACIFIC MISSILE TEST CENTER
ATTN CODE 3123, ABE J. GARRETT
ATTN CODE 1243, A. ANDERSON
POINT MUGU, CA 93042

COMMANDER
NAVAL SHIP ENGINEERING CENTER
PHILADELPHIA DIVISION
ATTN CODE 6772
PHILADELPHIA, PA 19112

COMMANDER
NAVAL SURFACE WEAPONS CENTER
ATTN CODE 413, CLAYTON MCKINDRA
ATTN CODE G-4, T. O'CONNOR
WHITE OAK, MD 20910

COMMANDER
NAVAL ORDNANCE STATION
ATTN CODE 5123C, K. ENGLANDER
INDIANHEAD, MD 20640

NAVAL SHIP RES & DEV CENTER
CODE 1619, K. READER
BETHESDA, MD 20084

NAVAL RESEARCH LABORATORY
ATTN S. SEARLES, 117 BG A68
WASHINGTON, DC 20375

NAVAL SEA SYSTEMS COMMAND
SEA0331H
ATTN A. CHAIKIN
WASHINGTON, DC 20362

COMMANDER
NAVAL WEAPONS CENTER
ATTN CODE 533, LIBRARY DIVISION
ATTN CODE 3636, C. BURMEISTER
CHINA LAKE, CA 93555

COMMANDER
AF AERO PROPULSION LABORATORY, AFSC
ATTN LESTER SMALL, AFWAL/POTC
WRIGHT-PATTERSON AFB, OH 45433

COMMANDER
AIR FORCE AVIONICS LABORATORY
ATTN AARA-2, RICHARD JACOBS
WRIGHT-PATTERSON AFB, OH 45433

DIRECTOR
AF OFFICE OF SCIENTIFIC RESEARCH
ATTN NE, GEORGE KNAUSENBERGER
BOLLING AFB, DC 20332

COMMANDER
AIR FORCE FLIGHT DYNAMICS LABORATORY
ATTN AFFDL/FGL, H. SNOWBALL
ATTN AFFDL.FER, R. J. DOBBEK
WRIGHT-PATTERSON AFB, OH 45433

COMMANDER
AF WEAPONS LABORATORY, AFSC
ATTN SUL, TECHNICAL LIBRARY
KIRTLAND AFB, NM 87117

COMMANDER
ARMAMENT DEVELOPMENT AND TEST CENTER
ATTN ADTC (DLOSL), TECH LIBRARY
ATTN DLMA, DAVID T. WILLIAMS
EGLIN AIR FORCE BASE, FL 32542

AIR FORCE FLIGHT TEST CENTER
6510 ABG/SSD
ATTN TECHNICAL LIBRARY
EDWARDS AFB, CA 93523

AF INSTITUTE OF TECHNOLOGY, AU
ATTN LIBRARY AFIT (LD),
BLDG 640, AREA B
ATTN AFIT (ENM), MILTON E. FRANKE
WRIGHT-PATTERSON AFB, OH 45433

HQ, AF SYSTEMS COMMAND
ATTN SGB, CPT GEORGE JAMES
ANDREWS AFB, DC 20334

ARGONNE NATIONAL LABORATORY
APPLIED PHYSICS DIV, BLDG 316
ATTN N. M. O'FALLON
9700 S. CASS AVE
ARGONNE, IL 60439

OAK RIDGE NATIONAL LABORATORY
CENTRAL RES LIBRARY, BLDG 4500N, RM 175
ATTN E. HOWARD
ATTN C. A. MOSSMAN
ATTN R. E. HARPER
P.O. BOX X
OAK RIDGE, TN 37830

DEPT OF NEW
PUBLIC HEALTH SERVICE
NATIONAL INSTITUTE OF HEALTH
ATTN. C. J. MCCARTHY
BLDG 13, RM 3W-13
BETHESDA, MD 20205

DEPARTMENT OF COMMERCE
NATIONAL BUREAU OF STANDARDS
ATTN JAMES SCHOOLEY, CHIEF,
TEMPERATURE SECTION
ATTN T. NEGAS, SOLID STATE
CHEMISTRY DIVISION
ATTN RAY DILS, RM B-254, BLDG 221
ATTN GEORGE BURNS, RM B-222, BLDG 221
WASHINGTON, DC 20234

DEPARTMENT OF COMMERCE
BUREAU OF EAST-WEST TRADE
OFFICE OF EXPORT ADMINISTRATION
ATTN WALTER J. RUSNACK
WASHINGTON, DC 20230

DEPARTMENT OF ENERGY
C-156, GTN (OART)
ATTN ROBERT ROBERTS
ATTN SANDY DAPKUNAS
ATTN T. K. LAU
WASHINGTON, DC 20545

DEPARTMENT OF ENERGY
F-317, GTN (COAL GASIFICATION)
ATTN JIM CARR
WASHINGTON, DC 20545

FEDERAL BUREAU OF INVESTIGATION
J. EDGAR HOOVER BLDG
ATTN ROBERT WILLIS
WASHINGTON, DC 20535

DEPARTMENT OF JUSTICE
IMMIGRATION AND NATURALIZATION SERVICE
425 "I" STREET NW
ATTN NEILL MCKAY
WASHINGTON, DC 20536

SCIENTIFIC LIBRARY
US PATENT OFFICE
ATTN MRS. CURETON
WASHINGTON, DC 20231

NASA AMES RESEARCH CENTER
ATTN MS 244-13, DEAN CHISEL
MOFFETT FIELD, CA 94035

NASA LANGLEY RESEARCH CENTER
ATTN MS 494, H. D. GARNER
ATTN MS 494, R. R. HELLBAUM
ATTN MS 185, TECHNICAL LIBRARY
HAMPTON, VA 23665

NASA SCIENTIFIC & TECH INFO FACILITY
ATTN ACQUISITIONS BRANCH
P.O. BOX 8657
BALTIMORE/WASHINGTON INTERNATIONAL
AIRPORT, MD 21240

UNIVERSITY OF ALABAMA
CIVIL & MINERAL ENGINEERING DEPT.
ATTN HAROLD R. HENRY
P.O. BOX 1468
UNIVERSITY, AL 35468

UNIVERSITY OF ARKANSAS
TECHNOLOGY CAMPUS
ATTN PAUL C. MCLEOD
P.O. BOX 3017
LITTLE ROCK, AR 72203

UNIVERSITY OF ARKANSAS
MECHANICAL ENGINEERING
ATTN JACK H. COLE, ASSOC PROF
FAYETTEVILLE, AR 72701

CARNEGIE-MELLON UNIVERSITY
SCHENLEY PARK
ATTN PROF W. T. ROULEAU, MECH ENGR DEPT
PITTSBURGH, PA 15213

CASE WESTERN RESERVE UNIVERSITY
ATTN PROF P. A. ORNER
ATTN PROF B. HORTON
UNIVERSITY CIRCLE
CLEVELAND, OH 44106

THE CITY COLLEGE OF THE CITY
UNIVERSITY OF NY
DEPT OF MECH ENGR
ATTN PROF L. JIJI
ATTN PROF. G. LOWEN
139th ST. AT CONVENT AVE
NEW YORK, NY 10031

CLEVELAND STATE UNIVERSITY
PENN COLLEGE OF ENGINEERING
ATTN PROF R. COMPARIN
CLEVELAND, OH 44115

DUKE UNIVERSITY
COLLEGE OF ENGINEERING
ATTN C. M. HARMAN
DURHAM, NC 27706

ENGINEERING SOCIETIES LIBRARY
ATTN HOWARD GORDON
ATTN ACQUISITIONS DEPARTMENT
345 EAST 47th STREET
NEW YORK, NY 10017

FRANKLIN INSTITUTE OF THE STATE
OF PENNSYLVANIA
ATTN KA-CHEUNG TSUI, ELEC ENGR DIV
ATTN C. A. BELSTERLING
20th STREET & PARKWAY
PHILADELPHIA, PA 19103

HUGHES HELICOPTERS
DIVISION OF SUMA CORPORATION
CENTINELA & TEALE STREETS
ATTN LIBRARY 2/T2124
CULVER CITY, CA 90230

IIT RESEARCH INSTITUTE
ATTN K. E. MCKEE
10 WEST 35th STREET
CHICAGO, IL 60616

JET PROPULSION LABORATORY
ATTN JOHN V. WALSH, MS 125-138
4800 OAK GROVE DRIVE
PASADENA, CA 91103

JOHNS HOPKINS UNIVERSITY
APPLIED PHYSICS LABORATORIES
ATTN MAYNARD HILL
ATTN THOMAS RANKIN
ATTN JOSEPH WALL
LAUREL, MD 20810

LEHIGH UNIVERSITY
DEPARTMENT OF MECHANICAL ENGINEERING
ATTN PROF FORBES T. BROWN
BETHLEHEM, PA 18015

LINDA HALL LIBRARY
ATTN DOCUMENTS DIVISION
5109 CHERRY STREET
KANSAS CITY, MO 64110

LOS ALAMOS SCIENTIFIC LAB
ATTN FRANK FINCH, MS 178
P.O. BOX 1663
LOS ALAMOS, NM 87545

MASSACHUSETTS INSTITUTE OF TECHNOLOGY
ATTN ENGINEERING TECHNICAL REPORTS,
RM 10-408
ATTN DAVID WORMLEY, MECH ENGR DEPT,
77 MASSACHUSETTS AVENUE
CAMBRIDGE, MA 02139

MICHIGAN TECHNOLOGICAL UNIVERSITY
LIBRARY DOCUMENTS DIVISION
ATTN J. HAWTHORNE
HOUGHTON, MI 49931

UNIVERSITY OF MISSISSIPPI
ATTN JOHN A. FOX
201 CARRIER HALL, DEPT OF MECH ENGR
UNIVERSITY, MS 38677

MISSISSIPPI STATE UNIVERSITY
DRAWER ME
ATTN C. J. BELL, MECH ENG DEPT
STATE COLLEGE, MS 39762

MISSISSIPPI STATE UNIVERSITY
DEPT OF AEROSPACE ENGINEERING
ATTN DAVID MURPHREE
MISSISSIPPI STATE, MS 39762

UNIVERSITY OF NEBRASKA LIBRARIES
ACQUISITIONS DEPT, SERIALS SECTIONS
ATTN ALAN GOULD
LINCOLN, NE 68508

UNIVERSITY OF NEW HAMPSHIRE
MECH ENGR DEPT, KINGSBURY HALL
ATTN PROF CHARLES TAFT
ATTN PROF DAVID LIMBERT
DURHAM, NH 03824

UNIVERSITY OF N. CAROLINA
INSTITUTE OF MARINE BIOMEDICAL RESEARCH
ATTN MICHAEL E. SHEEHAN
WILMINGTON, NC 28401

DEPARTMENT OF MECHANICAL ENGINEERING
NEW JERSEY INSTITUTE OF TECHNOLOGY
ATTN R. Y. CHEN
323 HIGH STREET
NEWARK, NJ 07102

OHIO STATE UNIVERSITY LIBRARIES
SERIAL DIVISION, MAIN LIBRARY
1858 NEIL AVENUE
COLUMBUS, OH 43210

OKLAHOMA STATE UNIVERSITY
SCHOOL OF MECH & AEROSPACE ENGR.
ATTN PROF KARL N. REID
STILLWATER, OK 74074

MIAMI UNIVERSITY
DEPT OF ENG TECH
SCHOOL OF APPLIED SCIENCE
ATTN PROF S. B. FRIEDMAN
OXFORD, OH 45056

PENNSYLVANIA STATE UNIVERSITY
ATTN J. L. SHEARER
215 MECHANICAL ENGINEERING BUILDING
UNIVERSITY PARK, PA 16802

PENNSYLVANIA STATE UNIVERSITY
ENGINEERING LIBRARY
ATTN M. BENNETT, ENGINEERING LIBRARIAN
201 HAMMOND BLDG
UNIVERSITY PARK, PA 16802

PORTLAND STATE UNIVERSITY
DEPT OF ENGINEERING AND
APPLIED SCIENCE
ATTN PROF P. I. CHEN
P.O. BOX 751
PORTLAND, OR 97207

PURDUE UNIVERSITY
SCHOOL OF MECHANICAL ENGINEERING
ATTN PROF. VICTOR W. GOLSSCHMIDT
ATTN PROF ALAN T. MCDONALD
LAFAYETTE, IN 47907

ROCK VALLEY COLLEGE
ATTN KEN BARTON
3301 NORTH MULFORD ROAD
ROCKFORD, IL 61101

RUTGERS UNIVERSITY
LIBRARY OF SCIENCE & MEDICINE
ATTN GOVERNMENT DOCUMENTS DEPT
SANDRA R. LIVINGSTON
NEW BRUNSWICK, NJ 08903

SYRACUSE UNIVERSITY
DEPT OF MECH & AEROSPACE ENGINEERING
ATTN PROFESSOR D. S. DOSANJH
139 E. A. LINK HALL
SYRACUSE, NY 13210

UNIVERSITY OF TENNESSEE
DEPT OF MECHANICAL ENGINEERING
ATTN PROF G. V. SMITH
KNOXVILLE, TN 37916

UNIVERSITY OF TENNESSEE SPACE INST
ENERGY CONVERSION DIVISION
ATTN MARY ANN SCOTT
TULLAHOMA, TN 37388

UNIVERSITY OF TEXAS AT AUSTIN
DEPT OF MECHANICAL ENGINEERING
ATTN A. J. HEALEY
AUSTIN, TX 78712

THE UNIVERSITY OF TEXAS AT ARLINGTON
MECHANICAL ENGINEERING DEPARTMENT
ATTN ROBERT L. WOODS
ARLINGTON, TX 76019

TULANE UNIVERSITY
DEPT OF MECHANICAL ENGINEERING
ATTN H. F. HRUBECKY
NEW ORLEANS, LA 70118

UNION COLLEGE
MECHANICAL ENGINEERING
ATTN ASSOC PROF W. C. AUBREY
MECH ENGR DEPT, STEINMETZ HALL
SCHENECTADY, NY 12308

VIRGINIA POLYTECHNIC INSTITUTE
OF STATE UNIV
MECHANICAL ENGINEERING DEPARTMENT
ATTN PROF H. MOSES

WASHINGTON UNIVERSITY
SCHOOL OF ENGINEERING
ATTN W. M. SWANSON
P. O. BOX 1185
ST. LOUIS MO 63130

WEST VIRGINIA UNIVERSITY
MECHANICAL ENGINEERING DEPARTMENT
ATTN RICHARD A. BAJURA
MORGANTOWN, WV 26505

WICHITA STATE UNIVERSITY
ATTN DEPT AERO ENGR, E. J. RODGERS
WICHITA, KS 67208

UNIVERSITY OF WISCONSIN
MECHANICAL ENGINEERING DEPARTMENT
ATTN FEDERAL REPORTS CENTER
ATTN NORMAL H. BEACHLEY, DIR,
DESIGN ENGINEERING LABORATORIES
1513 UNIVERSITY AVENUE
MADISON, WI 53706

WORCESTER POLYTECHNIC INSTITUTE
ATTN GEORGE C. GORDON LIBRARY (TR)
ATTN TECHNICAL REPORTS
WORCESTER, MA 01609

GARRETT PNEUMATIC SYSTEMS DIVISION
P.O. BOX 5217
ATTN GARY FREDERICK
ATTN TREVOR SUTTON
ATTN TOM TIPPETTS
ATTN C. ABBOTT
111 SOUTH 34th STREET
PHOENIX, AZ 85010

AVCO SYSTEMS DIVISION
ATTN W. K. CLARK
201 LOWELL STREET
WILMINGTON, MA 01887

BARNES ENGINEERING CO
ATTN FRED SWEIBAUM
30 COMMERCE ROAD
STANFORD, CT 06904

BELL HELICOPTER COMPANY
ATTN R. D. YEARY
P. O. BOX 482
FORTWORTH, TX 76101

BENDIX CORPORATION
ELECTRODYNAMICS DIVISION
ATTN D. COOPER
11600 SHERMAN WAY
N. HOLLYWOOD, CA 90605

BENDIX CORPORATION
RESEARCH LABORATORIES DIV.
BENDIX CENTER
ATTN C. J. AHERN
ATTN LAEL TAPLIN
SOUTHFIELD, MI 48075

BOEING COMPANY, THE
ATTN HENDRIK STRAUB
P. O. BOX 3707
SEATTLE, WA 98124

BOWLES FLUIDICS CORPORATION
ATTN VICE PRESIDENT/ENGR.
9347 FRASER AVENUE
SILVER SPRINGS, MD 20910

ROMALD BOWLES
2105 SONDRA COURT
SILVER SPRINGS, MD 20904

CHAMBERLAIN MANUFACTURING CORP
EAST 4th AND ESTHER STS
P. O. BOX 2545
WATERLOO, IA 50705

CONTINENTAL CAN DOMPANY
TECH CENTER
ATTN P. A. BAUER
1350 W. 76th STREET
CHICAGO, IL 60620

CORDIS CORPORATION
ATTN STEPHEN F. VADAS, K-2
P. O. BOX 428
MIAMI, FL 33137

CORNING GLASS WORKS
FLUIDIC PRODUCTS
ATTN R. H. BELLMAN
HOUGHTON PARK, B-2
CORNING, NY 14830

CHRYSLER CORPORATION
P. O. BOX 118
CIMS-418-33-22
ATTN L. GAU
DETROIT, MI 48231

JOHN DEERE PRODUCT ENGINEERING CENTER
ATTN V. S. Kumar
WATERLOO, IA 50704

ELECTRIC POWER RESEARCH INSTITUTE
3412 HILLVIEW AVENUE
P. O. BOX 10412
ATTN MS. M. ANGWIN,
P. M. GEOTHERMAL ENERG
PALO ALTO, CA 94303

FLUIDICS QUARTERLY
ATTN D. H. TARUMOTO
P. O. BOX 2989
STANFORD, CA 94305

FOXBORO CO
CORPORATE RESEARCH DIV
ATTN JAMES VIGNOS
ATTN J. DECARLO
ATTN JOHN CHANG
38 NEPONSET AVE
FOXBORO, MA 02035

GENERAL ELECTRIC COMPANY
SPACE/RESD DIVISIONS
ATTN MGR LIBRARIES, LARRY CHASEN
P. O. BOX 8555
PHILADELPHIA, PA 19101

GENERAL ELECTRIC COMPANY
KNOLLS ATOMIC POWER LABORATORY
ATTN D. KROMMENHOEK
SCHENECTADY, NY 12301

GENERAL MOTORS CORPORATION
DELCO ELECTRONICS DIV
MANFRED G. WRIGHT
NEW COMMERCIAL PRODUCTS
ATTN R. E. SPARKS
P. O. BOX 1104
KOKOMO, IN 460901

GRUMMAN AEROSPACE CORPORATION
TECHNICAL INFORMATION CENTER
ATTN C. W. TURNER, DOCUMENTS
LIBRARIAN
ATTN TED SORENSEN, MS B1535
ATTN JACK LEONARD, MS B1535
SOUTH OYSTER BAY ROAD
BETHPAGE, L. I., NY 11714

HAMILTON STANDARD
DIVISION OF UNITED AIRCRAFT CORP
ATTN PHILIP BARNES
WINDSOR LOCKS, CT 06096

HONEYWELL, INC
ATTN J. HEDEEN
ATTN W. POSINGIES
1625 ZARTHAN AVE
MINNEAPOLIS, MN 55413

HONEYWELL, INC
ATTN RICHARD STEWART, MS 200
1100 VIRGINIA DRIVE
FT WASHINGTON, PA 19034

JOHNSON CONTROLS, INC
ATTN WARREN A. LEDERMAN
ATTN GEORGE JANU
507 E MICHIGAN
MILWAUKEE, WI 53201

LEEDS & NORTHRUP CO
ATTN ERNEST VAN VALKENBURG
DICKERSON ROAD
NORTH WALES, PA 19454

MOORE PRODUCTS COMPANY
ATTN R. ADAMS
SPRING HOUSE, PA 19477

MARTIN MARIETTA CORPORATION
AEROSPACE DIVISION
ATTN R. K. BRODERSON, MP 326
P. O. BOX 5837
ORLANDO, FL 32805

MCDONNELL AIRCRAFT COMPANY
GUIDANCE AND CONTROL MECHANICS DIV
ATTN LOYAL GUENTHER
ST LOUIS, MO 63166

MCDONNELL DOUGLAS ASTRONAUTICS CO
PROPULSION DEPARTMENT
ATTN V. E. HALOULAKOS (A3-226)
ATTN J. D. SCHWEIKLE (A3-266)
5301 BOLSA AVENUE
HUNTINGTON BEACH, CA 92647

NATIONAL FLUID POWER ASSOCIATION
ATTN JOHN R. LUEKE
DIR OF TECH SERVICES
333 NORTH MAYFAIR ROAD
MILWAUKEE, MI 53222

NEOS, INC.
3711 AIR PARK ROAD
ATTN A. J. OSTEDIEK
LINCOLN, NE 68524

NORTHRUP CORP.
ELECTRONICS DIV., C3133, W/C
ATTN MR. DESMOND NELSON
2301 WEST 120th STREET
HAWTHORNE, CA 90250

PLESSEY AEROSPACE LTD
ATTN A. ROSENBERG
1700 OLD MEADOW ROAD
MCLEAN, VA 22102

PROCON, INC
ATTN HERB MARCH
OUP PLAZA
DES PLAINES, IL 60016

PROPULSION DYNAMICS
ATTN T. HOULIHAN
2200 SOMERVILLE R
ANNAPOLIS, MD 21401

RICHARD WHITE & ASSOCIATES
ELECTRO/MECHANICAL ENGINEERS
ATTN RICHARD P. WHITE
77 PELHAM ISLE ROAD
SUDBURY, MA 01776

ROCKWELL INTERNATIONAL CORPORATION
COLUMBUS AIRCRAFT DIVISION
P. O. BOX 1259
ATTN MARVIN SCHWIEGER
ATTN LOUIS BIAFORE
4300 E 59th AVENUE
COLUMBUS, OH 43216

SANDIA LABORATORIES
ATTN WILLIAM R. LUENBERGER, DIV 2323
ATTN JERRY HOOD
ATTN NED KELTNER
ATTN ANTHONY VENERUSO, DIV 4742
ALBUQUERQUE, NM 87185

SCIENCE APPLICATIONS, INC
8400 WESTPARK DR
ATTN J. ISEMAN
MCLEAN, VA 22102

SIKORSKY AIRCRAFT
NORTH MAIN STREET
ATTN J. R. SOEHLEIN
STRATFORD, CT 06602

STEIN ENGINEERING SERVICES, INC
5602 E. MONTEROSA
PHOENIX, AZ 85018

TRANS-TECH, INC
12 MEEM AVE
ATTN L. DOMINGUES
GAITHERSBURG, MD 20760

TRITEC, INC
ATTN L. SIERACKI
P. O. BOX 56
COLUMBIA, MD 21045

UNITED TECHNOLOGIES RESEARCH CENTER
ATTN R. E. OLSON, MGR FLUID
DYNAMICS LABORATORY
400 MAIN STREET
E. HARTFORD, CT 06108

VOUGHT CORPORATION
ATTN KELLEY FLING
P. O. BOX 225907
DALLAS, TX 75265

WESTINGHOUSE ELECTRIC CORP
1310 BEULAH RD
ATTN F. GOLDSCHMIED
PITTSBURGH, PA 15325

US ARMY ELECTRONICS RESEARCH
& DEVELOPMENT COMMAND
ATTN TECHNICAL DIRECTOR, DRDEL-CT

HARRY DIAMOND LABORATORIES
ATTN 00100, CO/TD/TSO/DIV DIRS
ATTN RECORD COPY, 81200
ATTN HDL LIBRARY, (3 COPIES), 81100
ATTN TECHNICAL REPORTS BRANCH, 81300
ATTN CHAIRMAN, EDITORIAL COMMITTEE
ATTN LEGAL OFFICE, 97000
ATTN CHIEF, 13000
ATTN CHIEF, 13400 (10 COPIES)
ATTN DRZEWIECKI, T (30 COPIES)